5-1-2017

Digital Laser Speckle Image Correlation

Mahshad Mosayebi
Southern Illinois University Carbondale, mahshad.mosayebi@siu.edu

DIGITAL LASER SPECKLE IMAGE CORRELATION

by

Mahshad Mosayebi

M.S., Southern Illinois University- Carbondale, 2017

A Thesis

Submitted in Partial Fulfillment of the Requirements for the

Master of Science Degree

Department of Mechanical Engineering and Energy Processing

Southern Illinois University Carbondale

May 2017

THESIS APPROVAL

DIGITAL LASER SPECKLE IMAGE CORRELATION

By

Mahshad Mosayebi

A Thesis Submitted in Partial

Fulfillment of the Requirements

for the Degree of

Master of Science

in the field of Mechanical Engineering

Approved by:

Dr. Tsuchin Philip Chu, Chair

Dr. Christopher Cooley

Dr. Rasit Koc

Dr. Mohammad Reza Sayeh

Graduate School
Southern Illinois University Carbondale
04/11/2017

AN ABSTRACT OF THE THESIS OF

Mahshad Mosayebi for the master of science degree in mechanical engineering, presented on April 11, 2017, at Southern Illinois University Carbondale.

TITLE: DIGITAL LASER SPECKLE IMAGE CORRELATION

MAJOR PROFESSOR: Dr. Tsuchin Philip Chu

This thesis examines the feasibility of combining Digital Image Correlation (DIC) with laser speckle based methods to form a new hybrid deformation measurement method called Digital Laser Speckle Image Correlation (DilSIC). Consequently, this method does not require any sample preparation and allows for the measurement of displacement of micro structures in addition to large displacements. In this technique, a coherent 30mW-632nm laser beam is expanded with 40X lens and then illuminated on the target surface to produce a fine, homogenous laser speckle pattern. Images were captured before and after deformation due to external load and the whole field displacement and strain were determined by the DIC method. This technique could measure displacement less than 30-μm with high accuracy when a 120mm × 80mm area of the surface was inspected. Up to 10% strain was measured by this technique with high accuracy during the whole range. Eventually the sub-surface crack was located successfully, which is a revolutionary achievement in NDT optical methods. This method was tested in different material, with different roughness. Aluminum sheet and rubber material were used mostly. This method could broaden the capability of displacement measurement and subsurface crack detection in wide range of materials.

DEDICATION

I would like to thank my brother, Mersad Mosaybi, who has never given up supporting and encouraging me to pursue my goals. And also for all his help in completing my master. This thesis is dedicated to him and also my parents who always inspire and motivate me in every step of my life even though they had to tolerate 7000 miles distance between us, for an unknown period.

ACKNOWLEDGEMENTS

I would like to thank to my advisor Dr. Tsuchin Philip Chu, Southern Illinois Carbondale (SIUC) for his unlimited helps, supports, brilliant ideas and being the best advisor who ever had.

I would like to thank Dr. Mohammad Reza Sayeh for providing me equipment and serving as committee member. Also I wanted to thank to Dr. Rasit Koc and Dr. Chris Cooley to be my committee members and for their help and input on this research work. . I would like to heartfully thank Mr. John Newman, President of Laser Technology Inc, PA, for providing us a Shearography LTI-2100 Device to carry out this research work and for all the technical expertise on LTI. I would like to thank Tim Attig for helping me build the DiLSIC test setup in the machine shop. I would also like to thank Ryan Spencer, Stephanie Venis, Albert Anthony Lyles, for their assistance.

TABLE OF CONTENTS

LIST OF TABLES

LIST OF FIGURES

CHAPTER 1

INTRODUCTION

This chapter discusses the idea of developing hybrid method by integrating a Digital Image Correlation (DIC) method with speckle patterns generated by a laser or laser based NDE system such as shearography. The reason of choosing Digital Image Correlation and laser based methods among all of the optical NDT techniques is described. In the literature review, the history and the background of what scientists and engineers have done to detect defects and strain using optical methods is described. In addition, the limits and possibilities of each method is revealed in this chapter. Finally, the scope and objective of the project is described.

1.1 Background

Engineers choose different methods to measure strain or to find defects based on the materials and experiment or inspection conditions. Additionally, feasibility, cost effectiveness, accuracy and rapidity are the other factors considered to find the best method for their investigation.

Optical methods become popular to measure surface strain mainly because of its non-destructive imaging characteristics with high precision and sensitivity. Among optical methods, Digital Image Correlation (DIC) and laser speckles interferometry was nominated to be used in measuring in-plane and out-of-plane displacement and finding surface defects. Both methods are non-contact and can be applied to very wide range of material, including metals and composites. Being capable of inspecting whole field at once placed them on the top of optical methods chart.

During recent decades, digital image correlation technique was used for strain mapping, material property recognition, and damage quantification. For example, NASA created a composite overwrapped pressure vessel (COPV) sample and used DIC to find defects. In figure 1, COPV is shown before and after being inspected with DIC method.

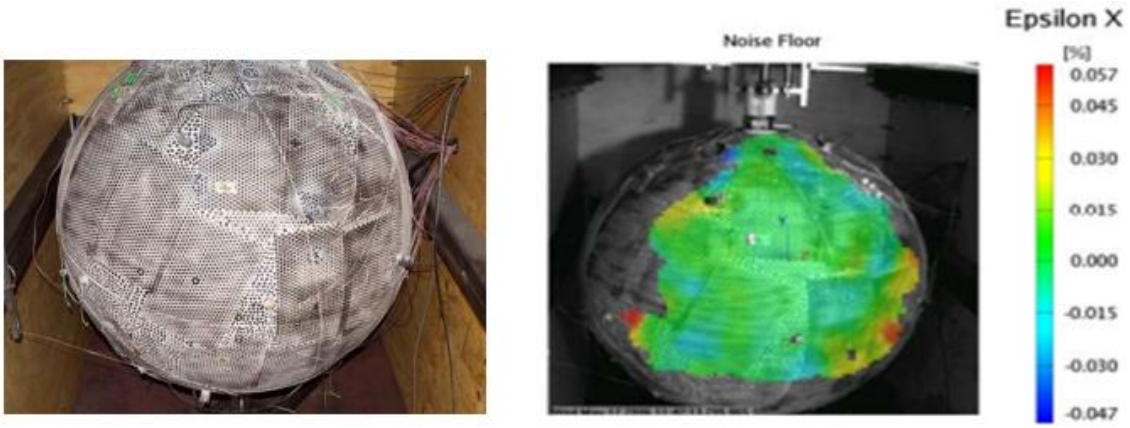

Figure 1: COPV with artifact speckle pattern for DIC (left) strain contours on COPV. Blue regions show the broken areas (right) [22]

Meanwhile, laser based techniques are widely used due to their high accuracy, feasibility and sensitivity. Traditional DIC uses artifact speckles to track deformation of a surface. This fact causes some limitations for the DIC technique. In many cases sophisticated speckles cannot be applied on the surface. Also, due to the speckle size, this technique is recommended to be used to inspect large deformation only. Achieving fine enough speckles is another challenge for engineers.

DIC owes its popularity for its simple setup and affordable equipment. On the other hand, the Laser Speckle Techniques are usually known for its high sensitivity. The other significant feature of laser speckle pattern technique is being able to be used in high temperature conditions or unreachable surfaces such as in vitro tissues. Advantages and limits of each method will be discussed in literature review.

The Laser speckles pattern technique is based on the interference of the wave front is divided by three main groups, Holography, Electrical Speckle Pattern Interferometry and Shearography. All of them use the common technique, Michelson interferometry. They interfere two beams together. One is illuminated laser beam by laser source directly while the other is diffracted from the target surface. This interference results in fringes called Young fringes. In all suggested laser based methods fringes are compared before and after applying load. Fringes can be incorporated either through real time or double exposure techniques. In double exposure, one image is captured first, before applying any deformation, then the second one is recorded after applying deformation in the same file, where here in real time technique first and second images (or fringes) are recorded at the time of occurrence. Therefore it cannot be post processed. Figure 2, shows an example of laser based techniques to find defects of an object. Fringes confine us to measure strain higher than 2% or displacement more than 1mm.

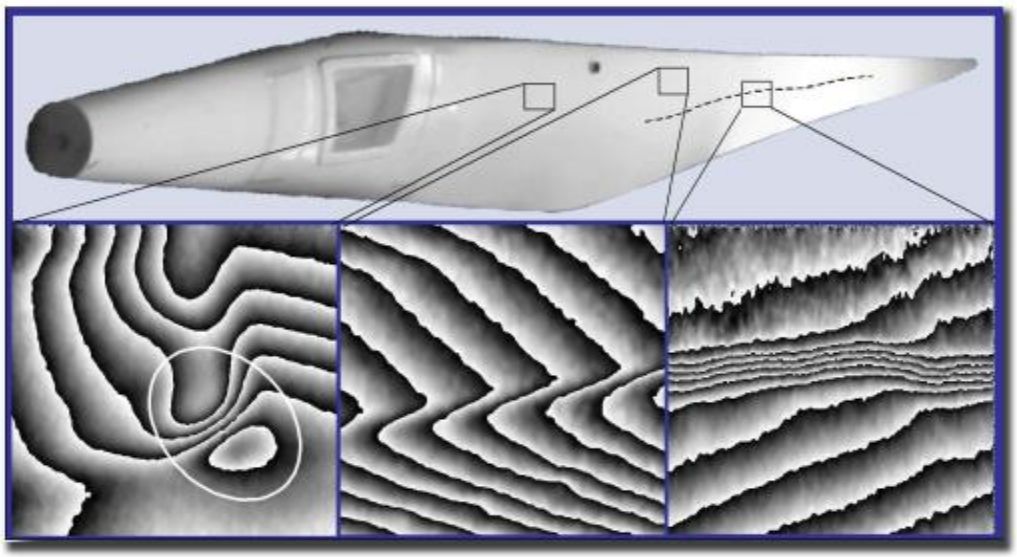

Figure 2: Using laser interferometry to find defects. Irregularities in fringes show defects [23]

The main advantage of this method as compared to its alternatives is the use of a laser speckle pattern instead of artifact speckles. Consequently, this method does not require any sample preparation, and allows for the measurement of displacement of micro structures in addition to the large displacements.

1.2 Literature Review

The commencement of optical strain measurement was 1975. In that year Khetan and Chiang were the first scientists who came up with the idea of measuring strain by one laser beam interferometry [11]. In this research the laser based methods' capability in strain measurement was validated for the first time. Before that, laser based methods were used to find defects only. Khetan used double exposure technique to record the results while he was applying deformation between two exposures. After introducing the new method of displacement, Phys used the laser-speckle gauge to measure the surface displacements in 1981 [11]. He used the laser speckle displacements which were found by photodiode array. Though his method was considered as a successful one on that time, the strain range that could be measured by his technique could not exceed 1mm. Digital Image Correlation (DIC) technique was pioneered by Chu et al. in the early 1980s for measuring surface displacements and deformation [1]. This method works with comparing pictures taken from speckle patterns on the sample, before (reference image), during and after the load applied. Speckle pattern tracking is the essence of these methods. DIC of speckle patterns has been used extensively in many applications to measure displacement components and deformation gradients of an object's surface due to deformation [2].

The basic correlation algorithm uses two image data sets, typically in the form of a speckle pattern, to extract deformation profiles from tiny changes in the images. On the other

word it uses speckle photography instead of speckle interferometry. As can be understood from above, the two methods are similar in recording image of two state of object, therefore they can be combined simply in order to achieve more accurate method which can eliminate many problems from each individual.

The DIC technique has been used for multiple applications. In order to measure the displacements or strain, Recorded files are incorporated and compared by the related software. The schematic of 2D DIC is shown in figure 3. Using multiple cameras permits to measure 3D deformation as well as 2D deformation. This achievement culminated in solving fracture problems. Three-dimensional DIC was used by NASA on Composite Overwrapped Pressure Vessels (COPVs) during pressure test [4]. They were successfully able to make accurate measurements of surface strain while monitoring COPV during pressure testing. DIC has also been used by NASA to monitor out of plane displacement and strain during buckling test on their full-scale launch vehicle shell structures [5]. These successful experiments using the DIC technique demonstrates the usefulness of the technique. The development and broad applications of DIC technique can be attributed to the rapid evolution of computers, CCD camera or recorders, and frame grabbers during the last decades. The economical and simple hardware combined with software make digital image acquisition and the solution to displacement field from acquired images easy and rapid.

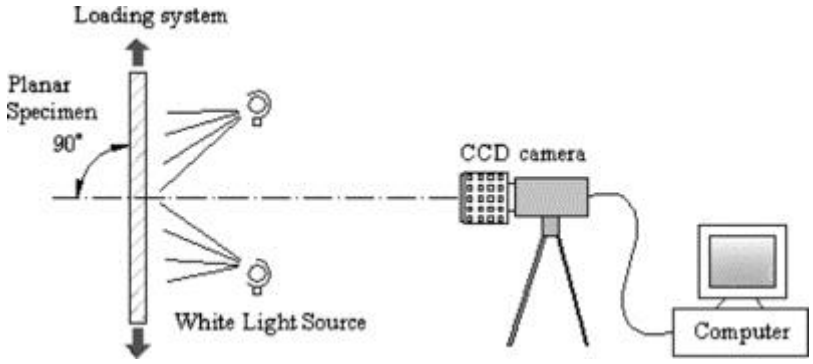

Figure 3: Schematic of 2D DIC [24].

Several experimental tests have been performed with the laser-speckle method or the Digital image correlation method. The laser-speckle method is interesting in terms of displacement measurement accuracy, 0.5 m, and spatial resolution, a point on the object covers 128 m 128 m. But this method has an important drawback: the speckle decorrelation that abruptly occurs in the presence of light variation, or excessive straining of the object, even for small displacement values. This does not allow us to measure strain values higher than 2%. Moreover this optical technique remains quite difficult and time consuming to apply.

In 2003, Schmit chose electronic speckle pattern interferometry (ESPI) as the best laser based method for strain measurement on that time and compared it with DIC. He revealed the results of that comparison in table 1.

Table 1: ESPI and DIC Comparison

ESPI	DIC
Interferometry	Photogrametery
Laser Speckle Pattern	Applied Stochastic Pattern
Highly Sensitive to vibration	Insensitive to vibration and rigid body motion
Sequentional	Simultaneous 3D measurement
Low dynamic range	High dynamic range
Real time display	Post Processing

Previously DIC were incorporated in some laser based techniques. Reu and Hansche Combined DIC and ESPI to measure 3D strain with simple setup than 3D ESPI. In their combination DIC was used to measure in-plane strain while ESPI measured out-of-plane strain [9].

1.3 Objectives

This research work is concentrated on identifying surface deformation on variable materials by applying laser speckle on them instead of applying artifact speckle pattern on surface. A proof of this method feasibility can help us compensate the error of laser based and white light DIC method individually. Also, this method does not need any sample preparation, due to this fact, it is broadening the range of material that can be tested under this technique. The goal of the proposed work is to investigative the feasibility of integrating a DIC method with current Laser Speckle Pattern technique to measure displacement and strain. This work has been done to show the application of DiLSIC method in industry. The following are the main

objectives of this research work: (1) acquire and setup laser speckle pattern system; (2) evaluate system performance; (3) conduct DiLSIC tests; and (4) develop DiLSIC algorithm.

1.4 Scope

This research work will incorporate Digital Laser Speckle Pattern Images (Images recorded by laser speckle photography technique) for the development of a new DIC system. By incorporating DIC image in Laser Speckle Pattern method we can achieve good quality fringe and more accurate results consequently. DIC can compensate any vibration of objects under study, even in methods which have the least sensitivity to vibration (such as shearography). Rubber material and metal samples shall be acquired for the proposed study. The proposed system will be capable of identifying and quantifying the distribution of strain and stress concentration in metal and composite structures. To achieve the above mentioned, DIC and laser speckle pattern technique shall be done separately when performing tensile and translation testing. The two techniques will then be combined for further experimentation.

1.5 Sequence of Presentation

In this thesis the possibilities and feasibility of laser based method and DIC integration was evaluated. Evaluation of this hybrid system was done by different experiments. In the first step the best set up for both DIC and laser system was recognized. After finding appropriate setup the first step of performance evaluation was done. In this step two images were captured from the sample without making any deformation or changing on its position. System was expected to show the zero displacement and strain on the sample at this case. This step helped us find the best subset radius and spacing. After achieving good result in pervious system, the objective was pursued through other steps. In the third step the performance and the sensitivity of

system to rigid body motion was examined called translation test. Fourth step showed the DiLSIC limits in strain/stress concentration recognition. Eventually the final step helped me evaluate the system capability to find subsurface defects. All of the results include, resulted FEA model, DIC results, DiLSIC and eventually integrated system with shearography device to show the capability of this method to be used in industry.

CHAPTER 2

THEORETICAL BACKGROUND

In this chapter**,** the theory behind both digital image correlation method and laser based technique. Then we will figure out how we can incorporate laser speckle images through DIC method.

2.1 Digital Image Correlation theory

DIC technique was developed based on image processing. Therefore, in order to become familiar with DIC principle, first the principle of image processing should be discussed. The part of image processing which helped DIC be developed will be explained briefly in this section.

Due to recent achievement of recording digital images help define image processing based on recording digital images on CCD cameras. Images captured before and after applying deformation. Reference image, the one which was captured before applying deformation, will be compared to the other images. This comparison leads us to find the displacement by the following process.

In the first step, captured images are imported to the related software. The software that was used in this project was NCORR. Ncorr is the software which can be used through MATLAB program. However the basic idea of all of the image processing software is the same. They define the imported image as two-dimensional function, f(x, y), where X and Y are spatial coordinates. An amplitude of f at any specific point is called intensity or gray level of that point. The gray level of each point is discrete quantities in a certain range. The X, Y coordinates are defined based on the image components called pixels. Pixel is the term used most widely to

denote the elements of a digital image. In traditional DIC the energy reflection and absorption of white light combined to generate the images used for DIC.

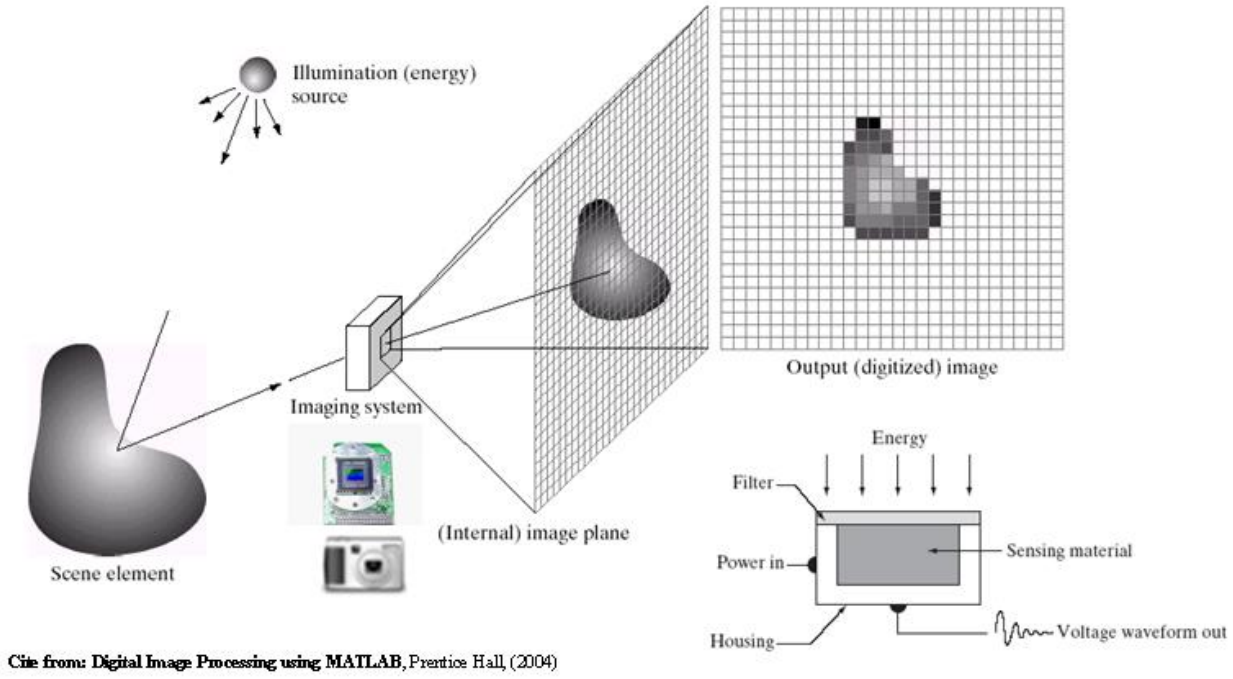

Figure 4: Digital Image Capture Theory

In figure 4, you can see how this system digitalizes the energy of each pixel and convert it to gray level. Digital quantity is obtained by digitalizing each sensor response.

As it was explained in the previous section the light intensity reflected from each pixel is shown by f (x, y). In order to prevent confusion the reflected light intensity from a pixel after deformation is shown by f*(x*,y*). It is assumed that f (x, y) and f*(x, y) are unique and one-to-one correspondence with the respective object surface. Therefore by tracking the intensities of pixels in each sub-images we can measure the surface displacement.

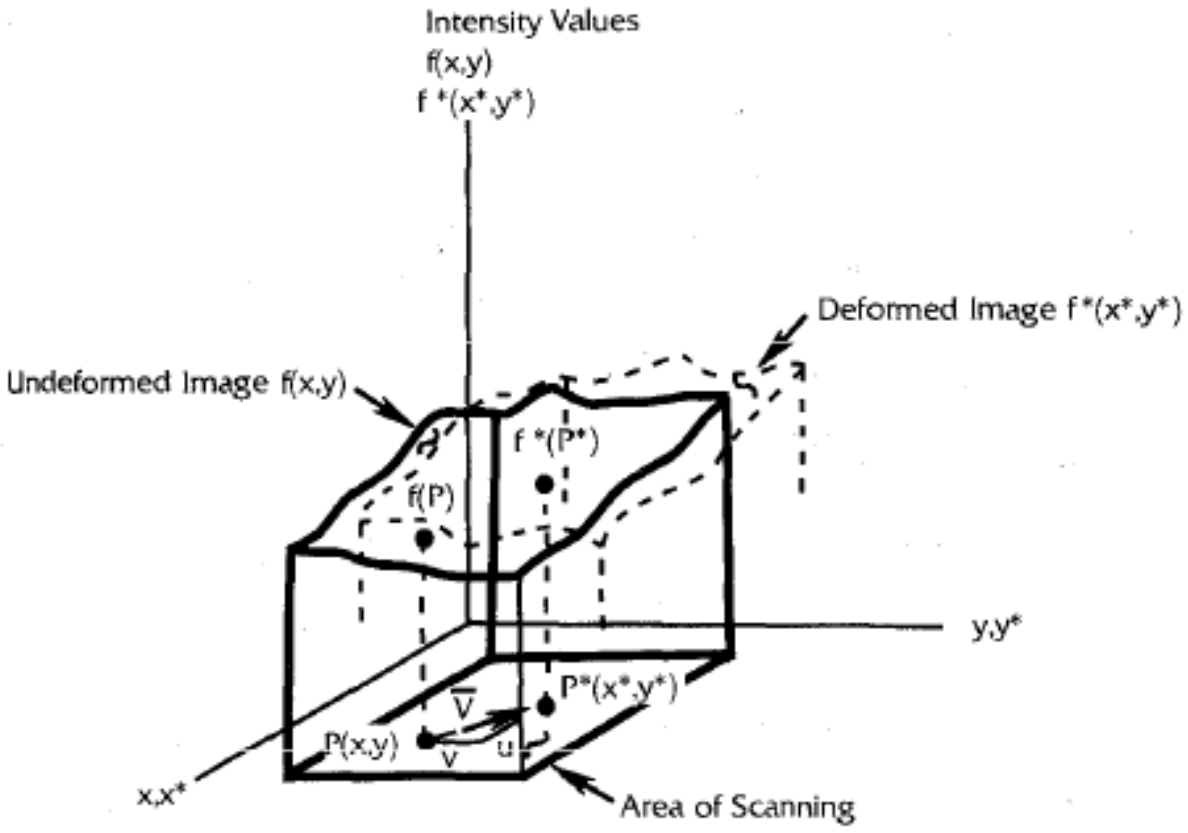

Figure 5: Gray level representation of deformed and non-deformed digital speckle images

As it was explained before, DIC claims the value of displacement by tracking the sub-images. In figure 6, this process is shown.

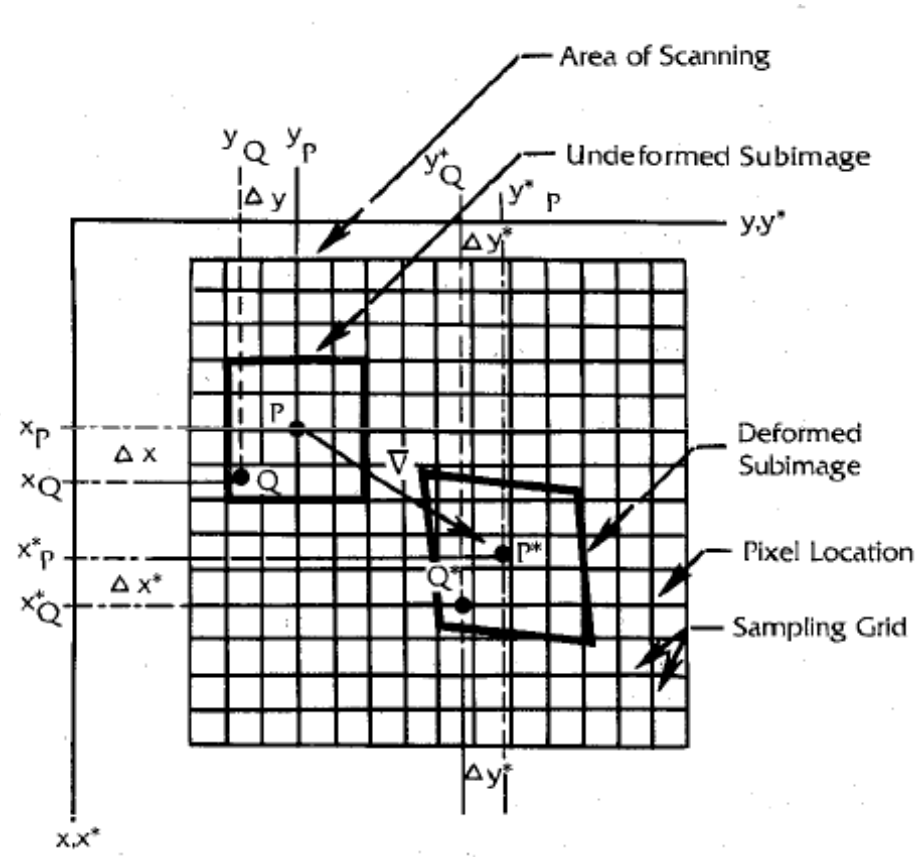

Figure 6: DIC tracks sub images

What has been explained so fare, was the basic theory of Digital image correlation. The software used during this project was Ncorr. This software was developed to calculate strain and displacement. Therefore it is necessary to become familiar with the calculation process of this

2.1.2 Software

Basically, the software is following almost the same process. It is tracking sub images called subsets. Subsets are a group of coordinate points. In figure 7, you can see how tracking subsets deformation can help us measure the displacements and strains. This deformation is assumed as the linear and first order in Ncorr, equation 1, shows the transformation of the subsets:

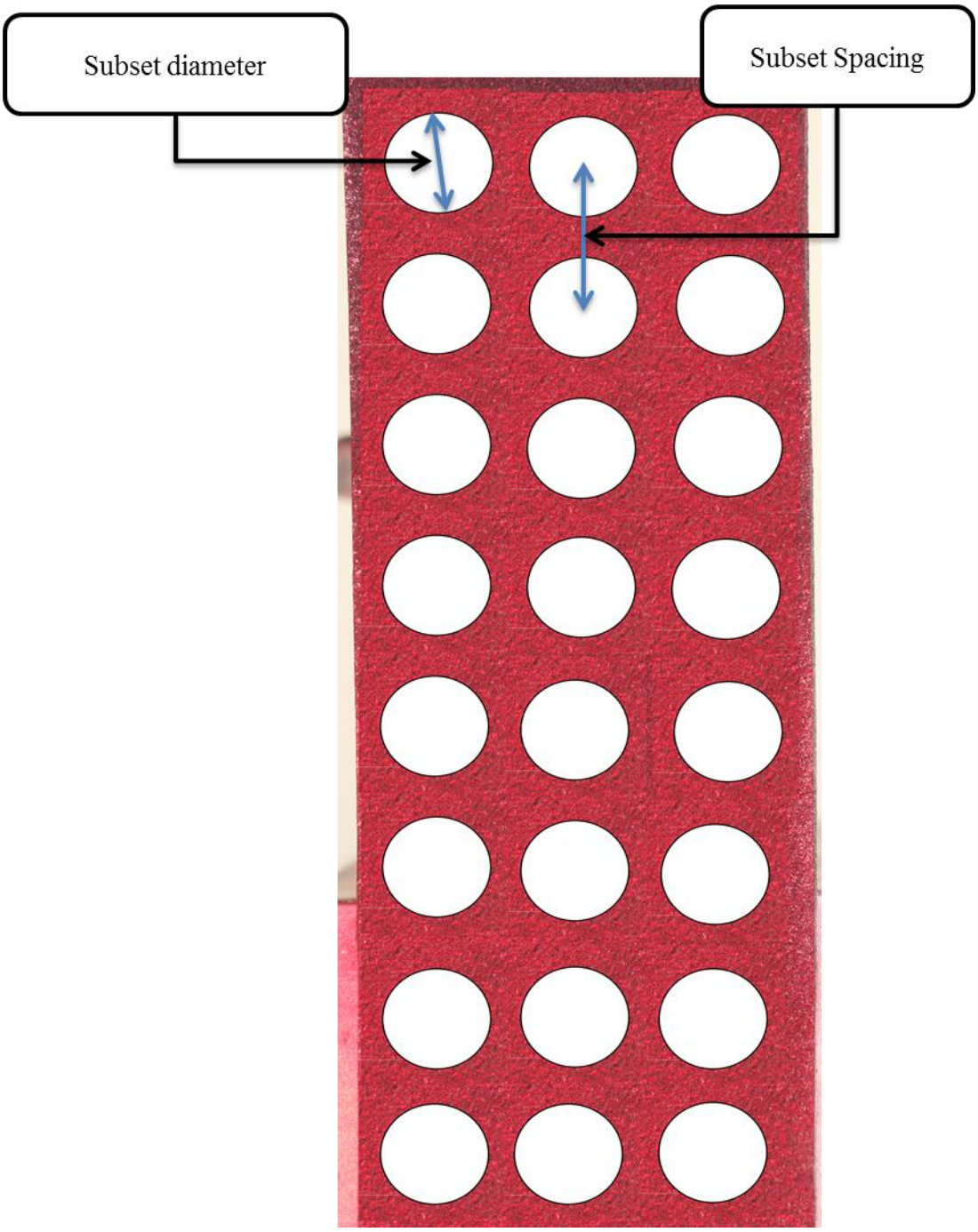

Figure 7: Subset Spacing and Subset Radius

$$\tilde{x}_{cur_i} = x_{ref_i} + u_{rc} + \frac{\partial u}{\partial x_{rc}}\left(x_{ref_i} - x_{ref_c}\right) + \frac{\partial u}{\partial y_{rc}}\left(y_{ref_j} - y_{ref_c}\right)$$

$$\tilde{y}_{cur_j} = y_{ref_j} + v_{rc} + \frac{\partial v}{\partial x_{rc}}\left(x_{ref_i} - x_{ref_c}\right) + \frac{\partial v}{\partial y_{rc}}\left(y_{ref_j} - y_{ref_c}\right) \qquad (i,j) \in S \qquad (1)$$

Where, i shows the initial step of the subset, c shows the center of the initial step and j shows the final step of the subsets.

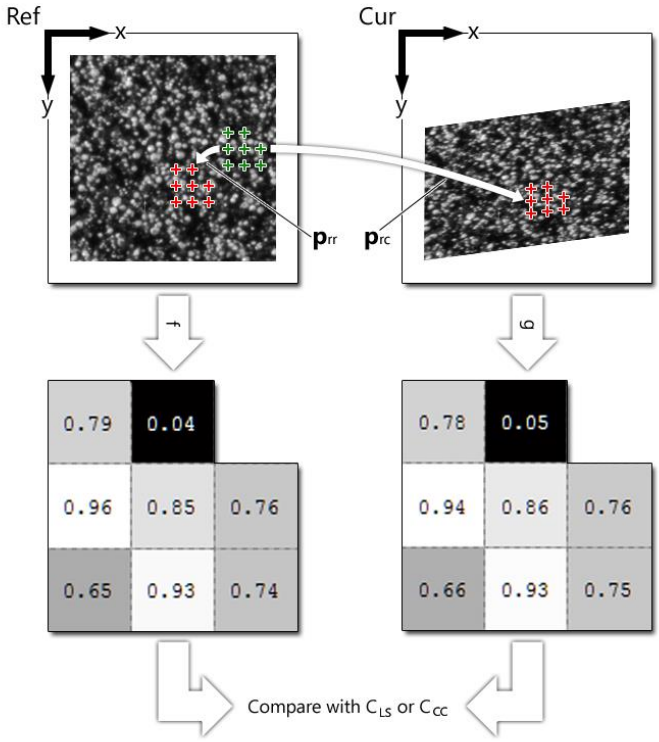

Figure 8: this image shows how Ncorr recognizes each subset and track them after deformation. Number shows the gray levels of coordinate points [23].

This software uses Gauss-Newton method in case that analytical solution is not available. As can be found from the equation 1, the displacement of the subset is determined by its center 0point.

Gray scale values are compared to find the correlation between current and reference images. The following equations are most commonly used in DIC [23].

Where f and g are the current and reference images and values are corresponded to point (x, y).

$$C_{CC} = \frac{\sum_{(i,j)\in S}\left(f\left(\tilde{x}_{ref_i}, \tilde{y}_{ref_j}\right) - f_m\right)\left(g\left(\tilde{x}_{cur_i}, \tilde{y}_{cur_j}\right) - g_m\right)}{\sqrt{\sum_{(i,j)\in S}\left[f\left(\tilde{x}_{ref_i}, \tilde{y}_{ref_j}\right) - f_m\right]^2 \sum_{(i,j)\in S}\left[g\left(\tilde{x}_{cur_i}, \tilde{y}_{cur_j}\right) - g_m\right]^2}}$$

$$C_{LS} = \sum_{(i,j)\in S}\left[\frac{f\left(\tilde{x}_{ref_i}, \tilde{y}_{ref_j}\right) - f_m}{\sqrt{\sum_{(i,j)\in S}\left[f\left(\tilde{x}_{ref_i}, \tilde{y}_{ref_j}\right) - f_m\right]^2}} - \frac{g\left(\tilde{x}_{cur_i}, \tilde{y}_{cur_j}\right) - g_m}{\sqrt{\sum_{(i,j)\in S}\left[g\left(\tilde{x}_{cur_i}, \tilde{y}_{cur_j}\right) - g_m\right]^2}}\right]^2 \quad (2)$$

Though this estimation is useful in several cases, usually full-field measurement is required. In order to have a full-field measurement, a region of interest must be selected first. After that, based on the sample geometry numbers of seeds would be selected. Seeds must be located in the appropriate position to track subsets. This seeds are being used as the leader of displacement tracking. Figure 9, describe how seeds are used for displacement measurement.

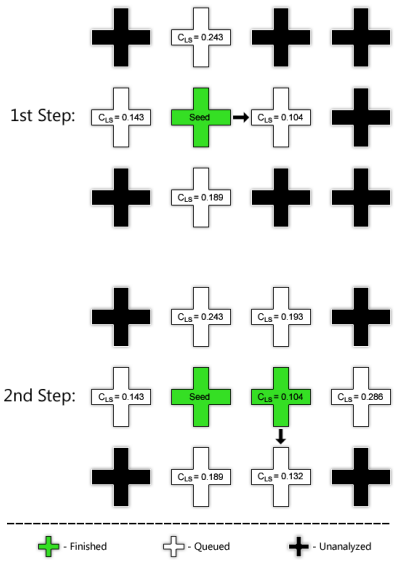

Figure 9: demonstration of RG-DIC algorithm. Algorithm is proceeded in lowest C_{LS} value [23].

Eventually they following equation are used by Ncorr to measure the in-plane strain:

$$E_{xx} = \frac{1}{2}\left(2\frac{\partial u}{\partial x} + \left(\frac{\partial u}{\partial x}\right)^2 + \left(\frac{\partial v}{\partial x}\right)^2\right)$$

$$E_{xy} = \frac{1}{2}\left(\frac{\partial u}{\partial y} + \frac{\partial v}{\partial x} + \frac{\partial u}{\partial x}\frac{\partial u}{\partial y} + \frac{\partial v}{\partial x}\frac{\partial v}{\partial y}\right) \quad (3)$$

$$E_{yy} = \frac{1}{2}\left(2\frac{\partial v}{\partial y} + \left(\frac{\partial u}{\partial y}\right)^2 + \left(\frac{\partial v}{\partial y}\right)^2\right)$$

2.2: Laser Speckle Based Theory

Laser speckles pattern technique is based on the interference of the wave front is divided by three main groups, Holography, Electrical Speckle Pattern Interferometry and Shearography. All of them use the common technique. They interfere two beams together. One is from laser source directly while the other is diffracted from the target surface. This interference results in fringes called Young fringes. In all suggested laser based methods fringes are compared before

and after applying load. Fringes can be incorporated either through real time or double exposure technique. In double exposure, first image is captured before any changes then the second one is recorded in a different file. Where in real time technique first and second images (or fringes) in the same file.

When the scattering surface is illuminated by a coherent laser beam, random speckle pattern is created called laser speckle pattern. In figure 10 laser speckle pattern can be seen on a rubber sample.

Figure 10: Laser speckle pattern on a rubber sample

The interferometry of laser speckle pattern before and after applying deformation created fringes shown in figure 11. These fringes are called Young's fringes. Young's fringes are used to measure in-plane and out of plane displacement.

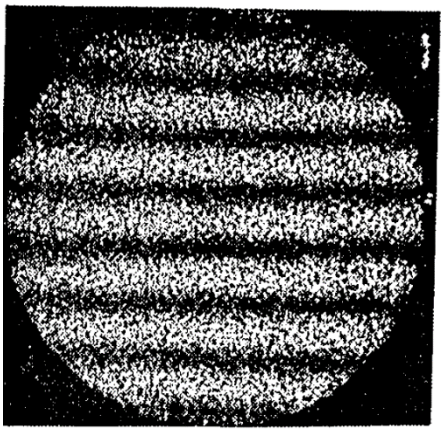

Figure 11: Young's fringes created by interferometry of two laser speckle pattern

Young fringes can be viewed either in real time or in double exposure technique. While the double exposure one is really time consuming. The intensity distribution (I) in the spatial domain is described as equation (4).

$$I(x_s, y_s) = I_0(x_s, y_s) + \left[4\cos^2\left(k\frac{x_s d_{ix} + y_s d_{iy}}{2z}\right)\right] I_1(x_s, y_s) \qquad (4)$$

X_s and y_s are coordinates on the viewing screen. K is the wave number, λ is the wavelength and z is the distance between specklegram and the viewing screen. I_o is the non-diffracted laser beam on the center of screen.

Any phase difference between the exposures causes the change detailed intensity distribution unless the changes are a multiple of 2π. To measure the out of plane displacement by Young's fringes, the equation (5) is used. Where in this equation, d is displacement, α and β are observation and illumination angles and N is the number of fringes [10].

$$d = \lambda N/(\cos\alpha + \cos\beta) \qquad (5)$$

The three main techniques of laser based methods are Holography, Electrical Speckle Pattern Interferometry (ESPI) and Shearography. Later the theory, limits and possibilities of each method will be discussed.

2.2.1 Holography:

In the figure 12, you can see the basic setup of Holography. Holography involves the capture and subsequent reconstruction of a light wave front emanating from an object. This wave front contains both amplitude and phase information, such as all of the laser based methods, which upon reconstruction will yield intensity and spatial differences in the image. Holographic Interferometry takes this process further by capturing a second image of the illuminated object in the same recording medium (usually a photographic film emulsion) after applying deformation by any means. Any changes due to environment changes or applied direct loading will produce a different light wave front (due to dimensional changes) that gets captured in the same photographic emulsion. The two light wave fronts will now interfere with each other and when the photographic film is processed and is illuminated by the reconstructing (reference) light beam the image that appears will be that of the object with zebra like lines superimposed on it. Beam splitter is used to build Michelson interferometry which uses the reference laser beam and the diffracted one. The lines (fringes) form what is known as the interference pattern which is a contour map of the deformation of the object's surface as a direct result of its perturbation by the heat applied or mechanical means as described above. Any changes on the surface will cause the significant irregularities in fringe patterns. As can be seen in figure 13, irregularities happened due to deforming surface.

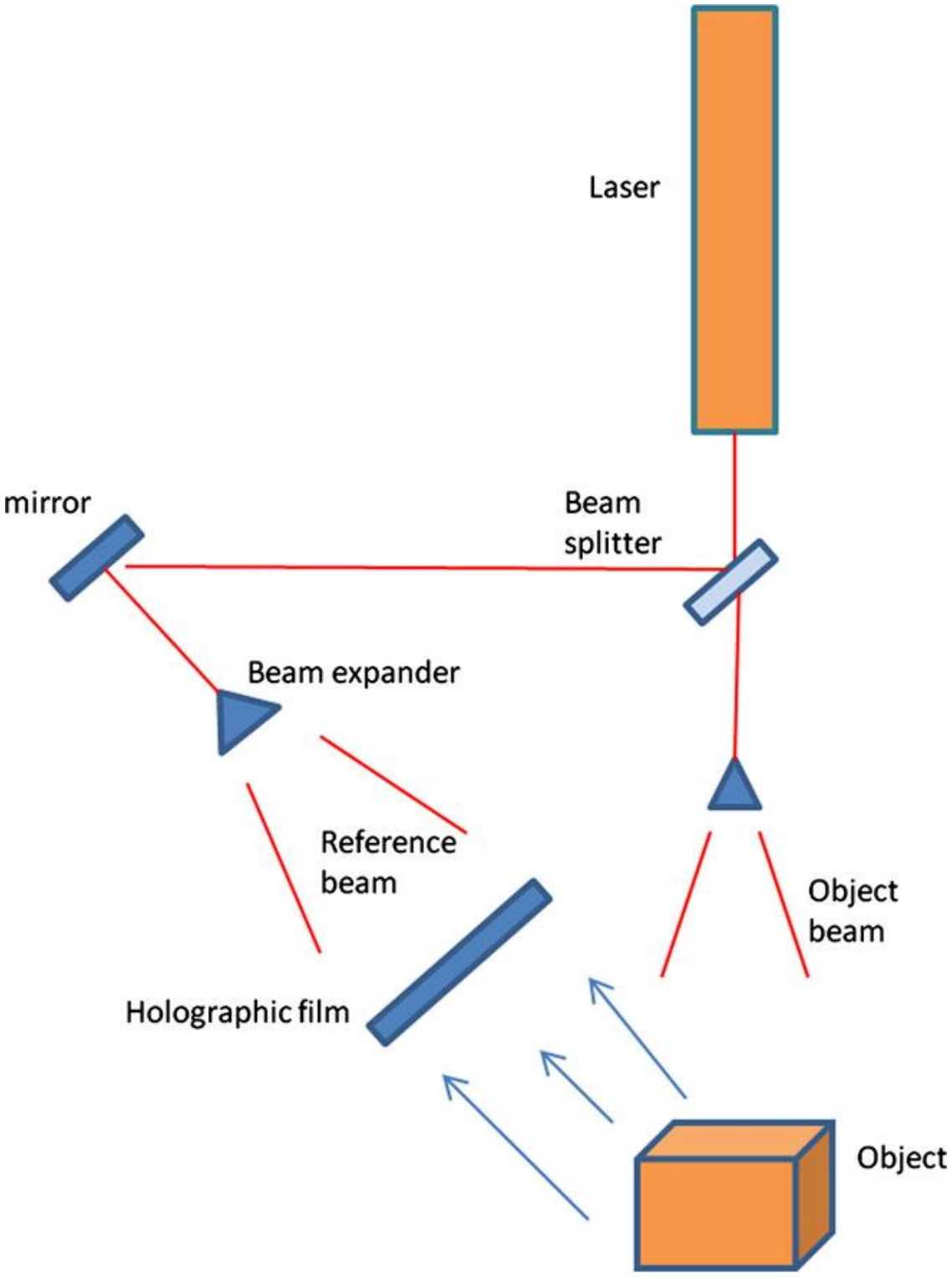

Figure 12: Holography Setup [10]

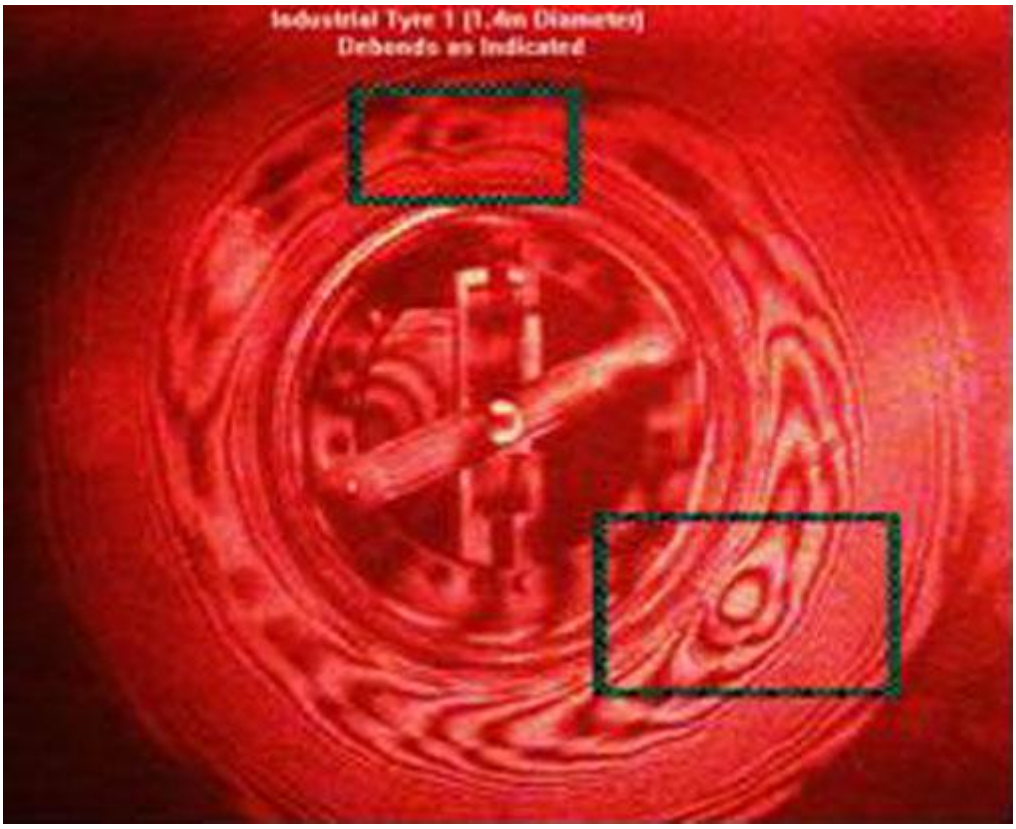

Figure 13: Typical Holography results. The outline indicates location of debond in the casing. [10]

2.2.2 Electronic Speckle Pattern Interferometry:

Basically ESPI is following the same instruction as holography, while instead of using holography film to record the results. This fact can speed up the process to a great deal. ESPI is the best laser interferometry based technique to measure the strain, especially for the out of plane deformation. Usually this technique is used for strain measurement when we have very small displacements. In figure 14, the general setup of ESPI is depicted. Since this technique has the same hypothesis as holography, the similar results are expected. ESPI result is shown in figure 15, 16.

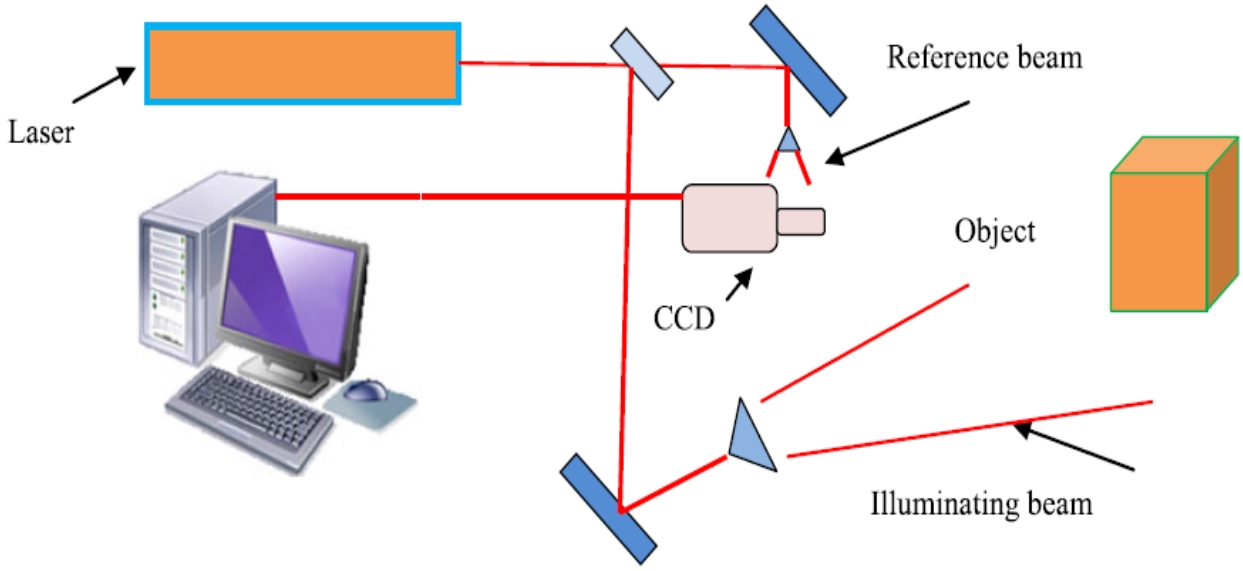

Figure 14: Typical ESPI out of plane displacement measurement setup [10]

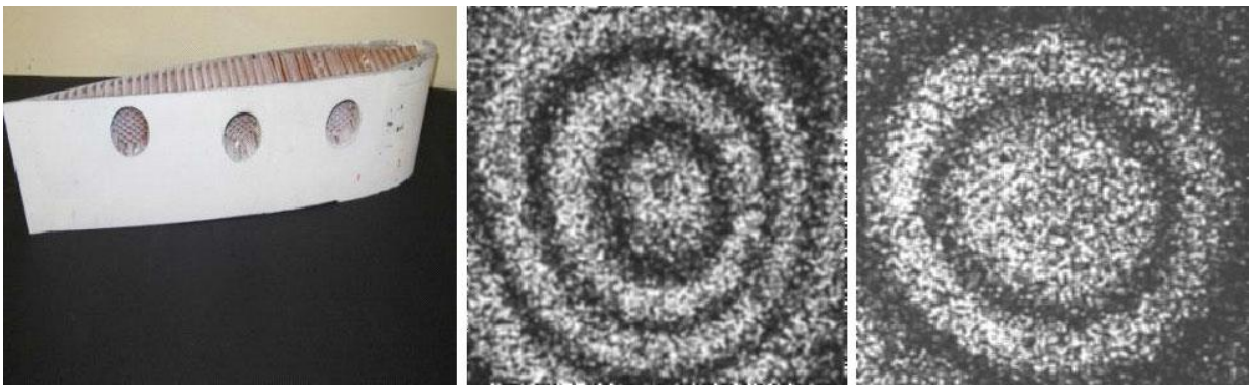

Figure 15: typical ESPI results from the defects on a helicopter rotor blade section obtained through heating [10]

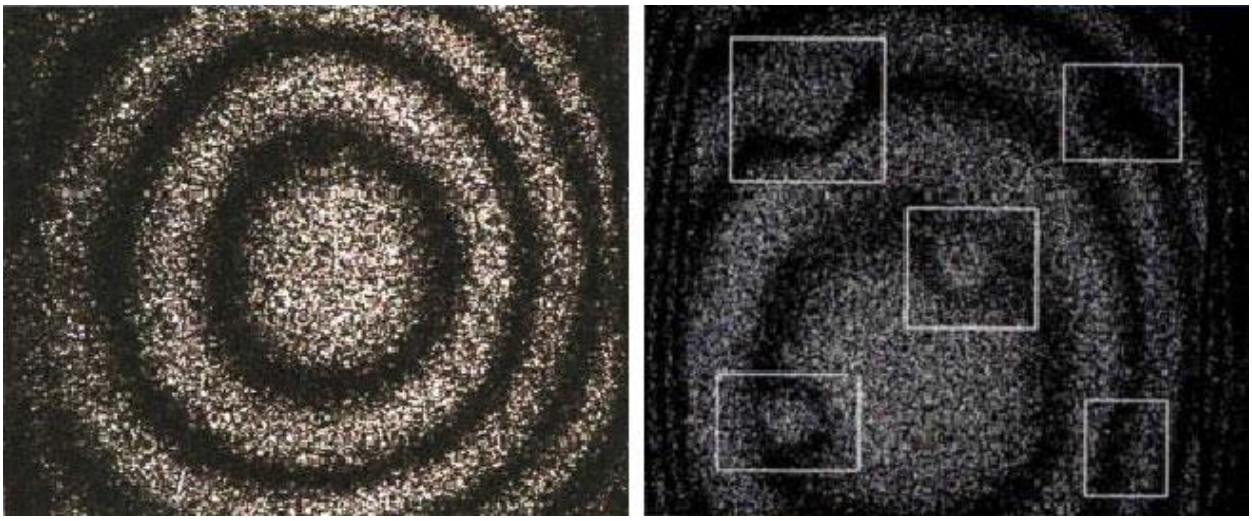

Figure 16: Impact damage revealed on a UAV wing specimen through ESPI [10]

2.2.3 Digital Shearography

Shearography is another laser based method which could be developed by advancing in digital cameras and CCDs. This portable technique is based on laser speckle pattern interferometry too. It detects the flaws and defects as a localized disturbance in the fringe pattern depicting the gradient of the surface displacement on the test specimen. In figure 18 , the typical shearography setup is depicted.

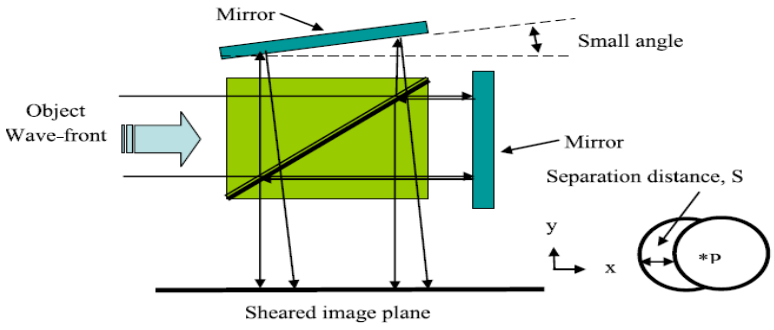

Figure 17: Image shearing device base on Michelson interferometer [10]

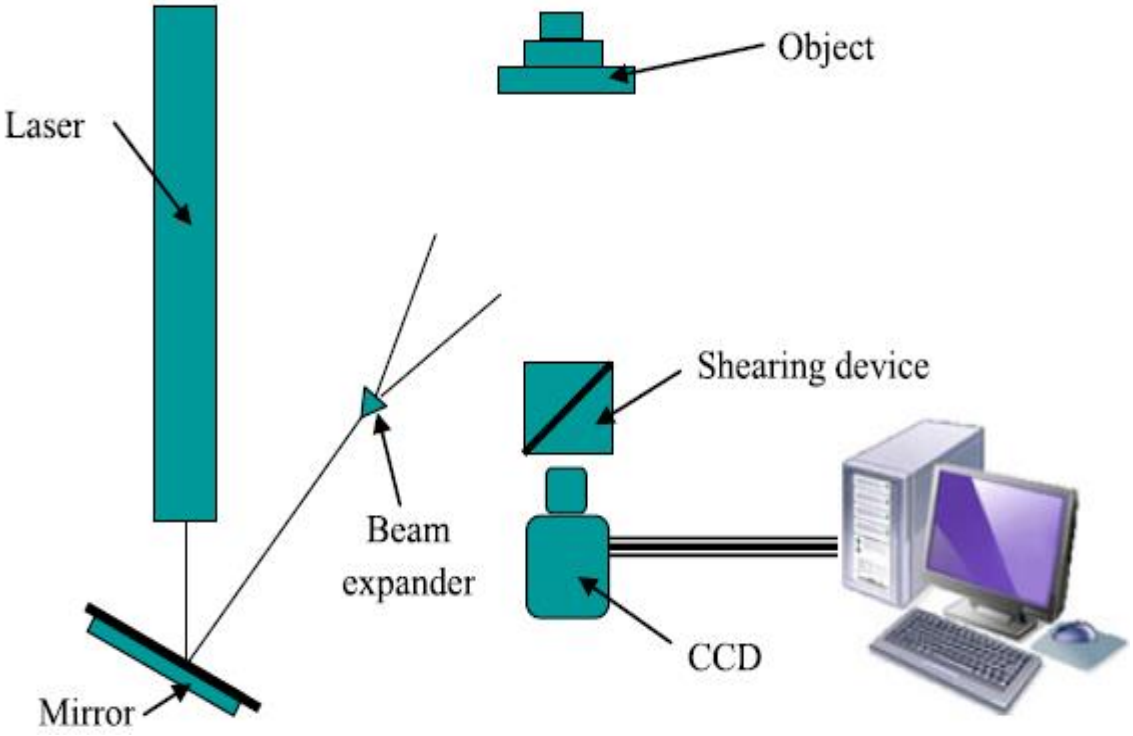

Figure 18: Typical Laboratory Shearography System [10]

This technique requires the image shearing device (figure 17). Shearing device duplicates images. The symmetric axis of the shearography images is the shearing vector which can be adjusted by the user.

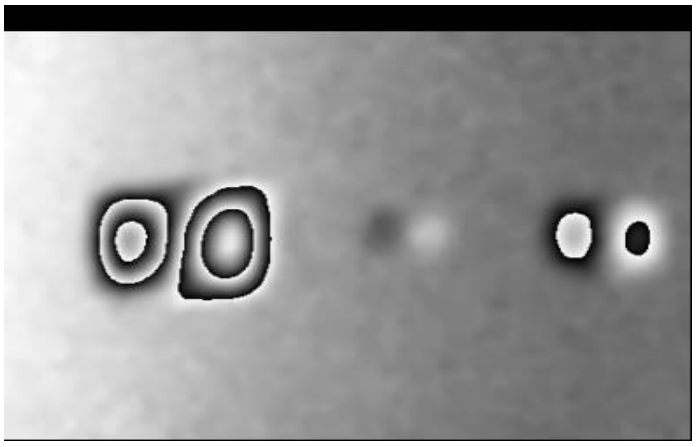

Figure 19: Typical shearography results [10]

Shearography is less sensitive to vibration of the environment in compare to other laser based method. This state of art technique is usually used in aerospace application. Not-contact, accurate and rapid analysis made it very popular recently. Later in this project, the limits and possibilities of all methods will be investigated.

CHAPTER 3

GENERAL SETUP

Five different experiments including rigid body translation, tensile strain, stress concentration around a hole, and subsurface defect detection were performed. In this chapter the setup of all of the experiments is described. The material properties and geometry of the samples are provided. The setting used in the software (Ncorr) is also explained.

3.1 Hardware Setups

Different samples were used in different parts. In figure 20, the samples used in translation test is depicted. Aluminum sheets have the same material properties. This experiment was done with the rubber sample at its last step. Since it was a rigid body motion the geometry of samples were not an effective factor, it was not described.

Figure 20: Translation test samples. Left: aluminum sheet with texture, middle: white painted aluminum sheet right: Rubber

The rest of the experiments were done with the rubber sample. Different geometry used in different experiments. Figure 21 shows all of the samples used in the rest of the procedure.

The top and the middle samples were used for both DiLSIC and DIC. In one side of them there are fine artifact speckle patterns for DIC, while on the other side laser speckle patterns were illuminated. Depth of samples is 3mm. In the sample with crack, the depth of the crack is 1mm.

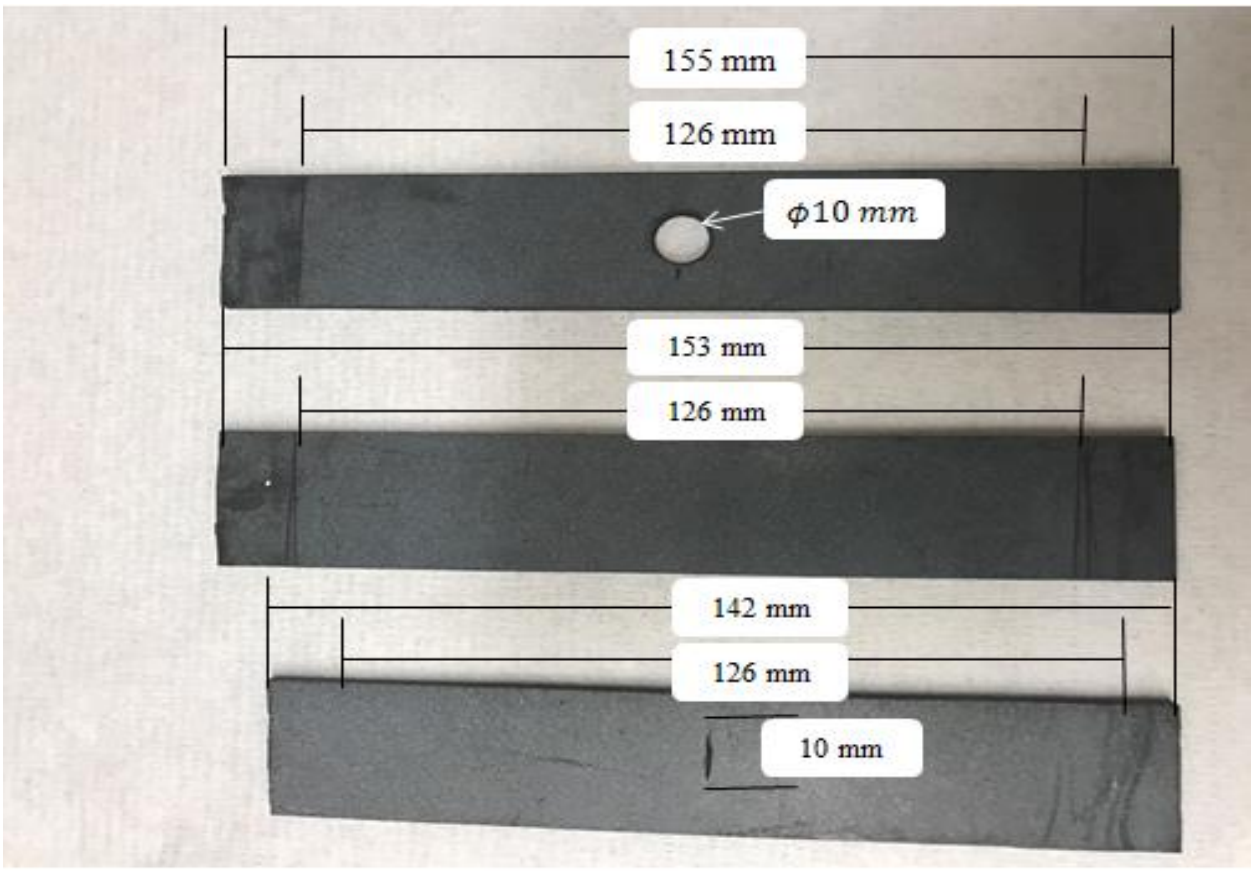

Figure 21: samples used in strain concentration tests (top), regular strain mapping (middle) and crack detection (bottom)

The first experiment was translation test. In Figure 22, the setup used in translation test is depicted.

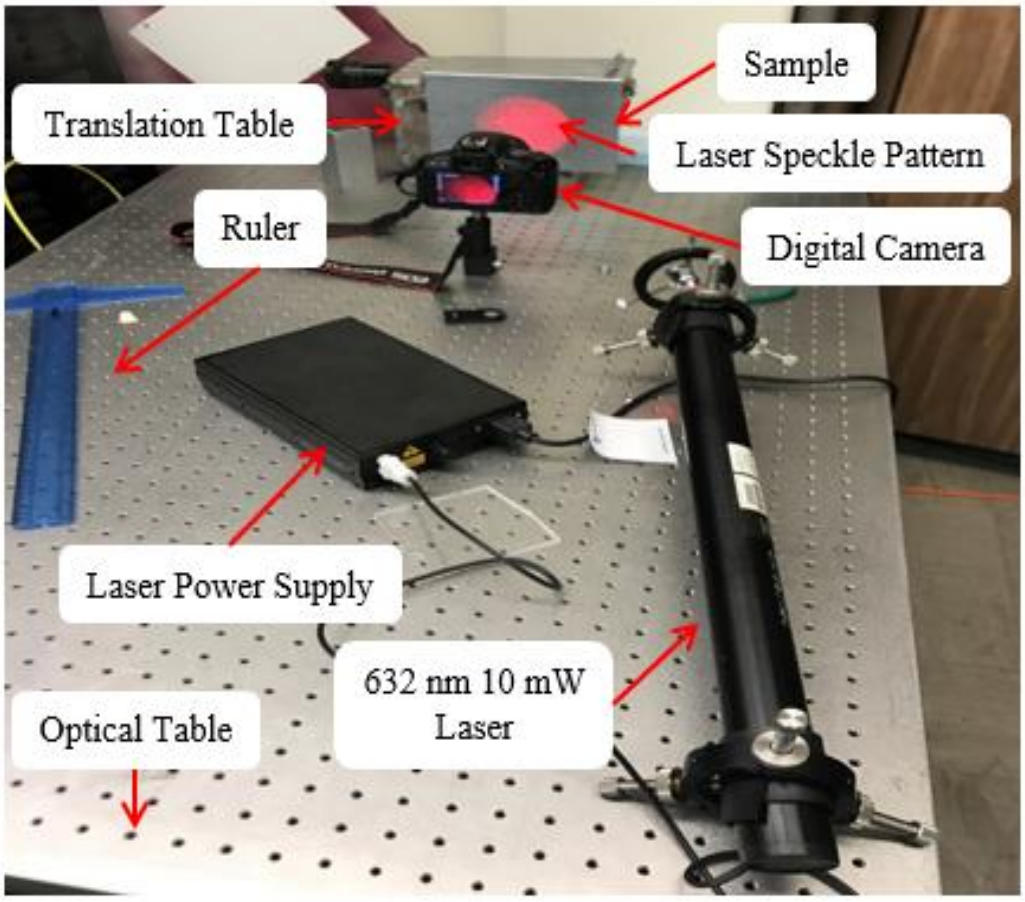

Figure 22: Translation Test setup

As shown in Figure 22, translation table is designed for translation test. It has two degree of freedom which allows users to move their sample either in x or z direction. The precision of the measurement is 0.0001in. The optical table is Newport I2000 series vibration isolation one which was used for setting up all instruments for the experiments. A red coherent laser was used during the whole process to generate laser speckles. Wavelength of the laser is 632.8nm and the power is 30mW. The distance between the expander lens and the target surface was 62cm while the illumination beam was about 35deg related to the target surface. A 40X lens was used to expand the laser beam.

A digital camera was used to record DIC images. It was a T5I Cannon camerawith an EFS 55mm lens.

3.2 Software Setup

3.2.1 Camera setup

The optimum aperture size and exposure time of the camera should be chosen in order to have the highest contrast in the images. To evaluate the contrast of the image, histogram of the images were used. The widest range histogram is considered as the best one. Figure 23 shows the histogram of the optimum camera setup. Where the exposure time was 1.3 sec and aperture size was 8.

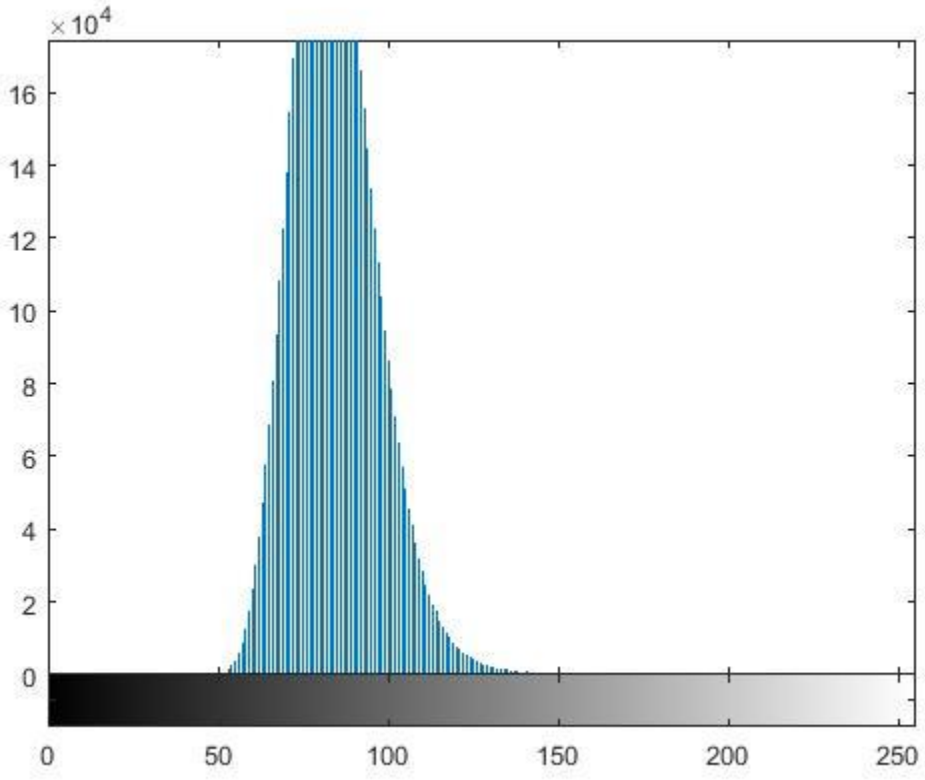

Figure 23: histogram of chosen camera setup for the exposure time of 1.3sec and aperture size of 8

3.2.2 Shearography Setup

To evaluate the feasibility of integration of DIC and laser based methods, Laser LTI-2100 including its integrated laptop, two red laser sources, heater lamp, shearing device, shearography camera and etc. distance between shearography camera and the target surface was 23cm. The length of shearing vector was zero to give us the regular image without any interferometry. But in this setup, some noises and irregularities occurred. Therefore the duplicated image was removed from the region of interest. The camera was focus. The heater lamps were off during the process.

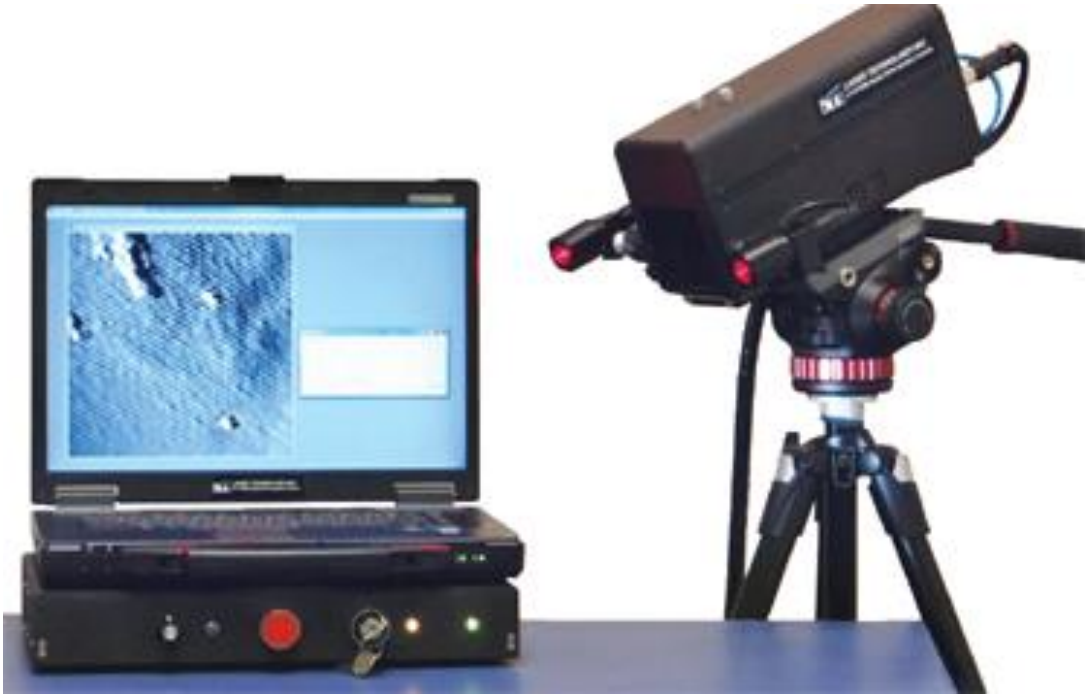

Figure 24: LTI-2100- Shearography device [25]

3.2.3 Ncorr setting

The Region of Interest (ROI) was chosen based on the critical area. In the strain concentration experiment, the area around the hole was crucial for us. In the crack detection experiments the area with probability of crack was selected. Since it was a sub-surface crack, the whole part was selected. While in the translation test and uniform tensile test on the regular sample ROI did not have an important role. Figure 25 shows the ROI of each steps.

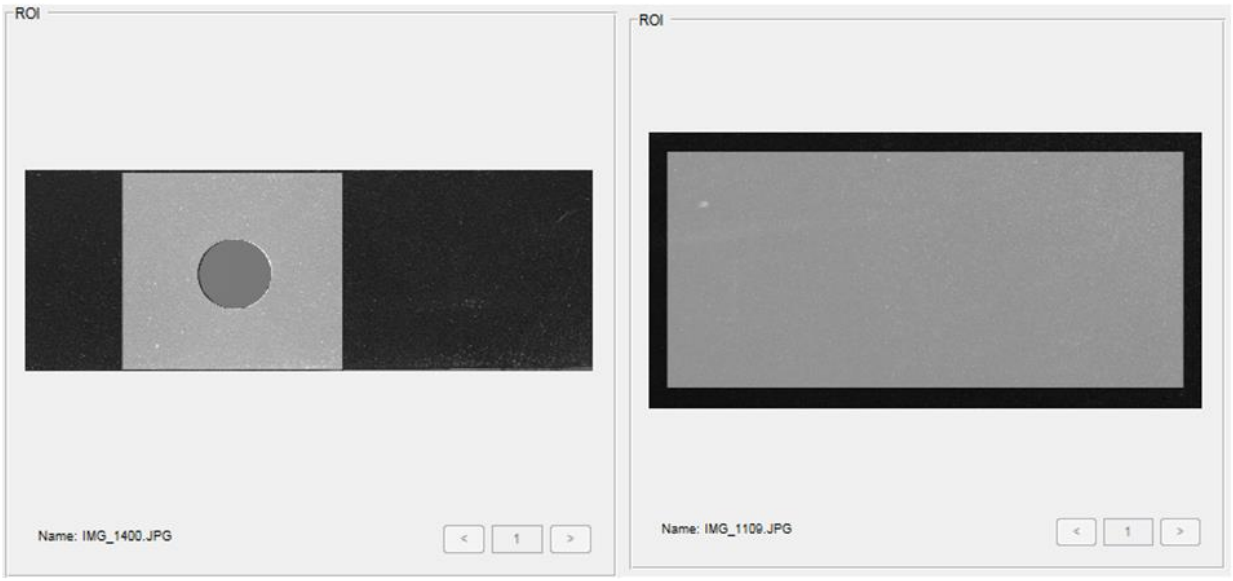

Figure 25: ROI of the strain concentration test (left) and ROI for crack detection (right)

In this part DIC parameters such as subset radius and subset spacing must be determined. In order to find the optimum values of subset radius and subset spacing, two images captured after each other without making any displacement or deformation between exposures. By this way, figure 26, was resulted for aluminum and Figure 27 for rubber. The minimum subset radius with the minimum range of displacement (because actual applied displacement was zero) is considered as the best one. Based on this assumption, radius equals to 20 was selected. The subset spacing was 1.

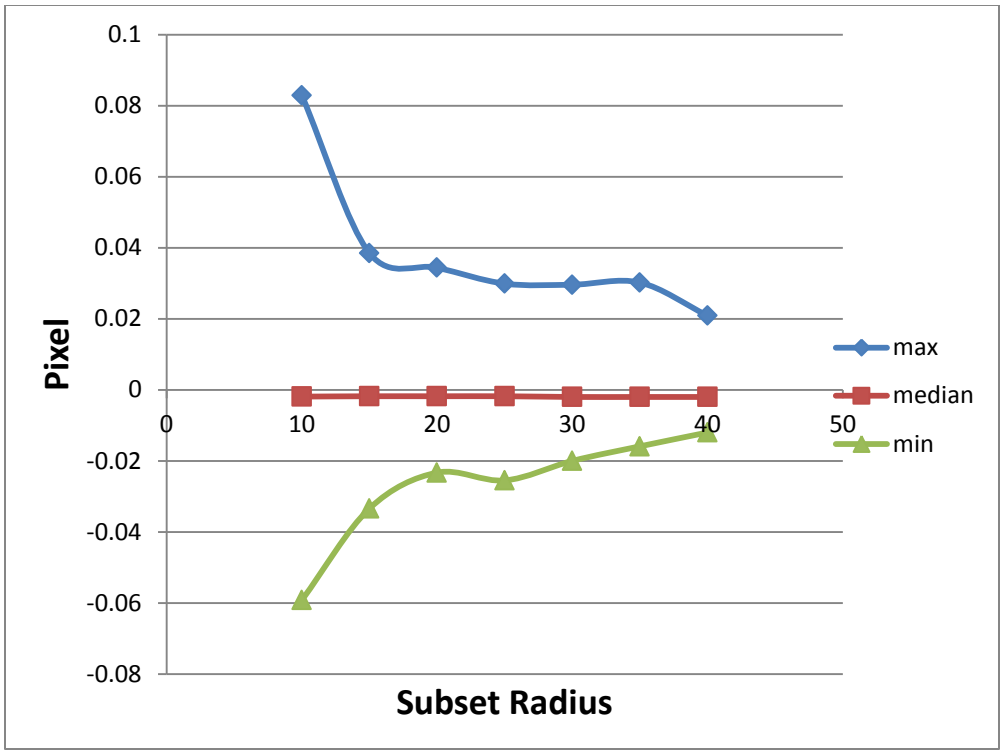

Figure 26: subset radius optimization for metal

Table 2: subset radius optimization for metal

radius	max	median	min
10	0.0829	-0.0019	-0.0592
15	0.0385	-0.0018	-0.0334
20	0.0344	-0.0018	-0.0233
25	0.0299	-0.0018	-0.0255
30	0.0296	-0.002	-0.02
35	0.0302	-0.002	-0.0159
40	0.0209	-0.002	-0.012
45	High Deco	0	0

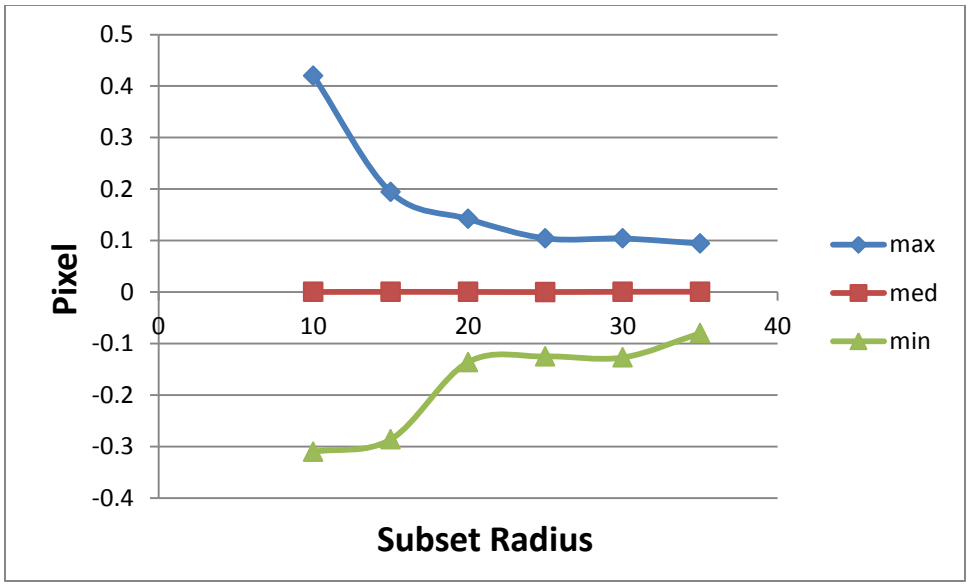

Figure 27: subset radius optimization for rubber

Table 3: subset radius optimization for rubber

r	max	med	min
10	0.42	0.0002	-0.31
15	0.194	0.0005	-0.286
20	0.142	0.0003	-0.136
25	0.1043	0.0001	-0.125
30	0.104	0.0006	-0.127
35	0.0943	0.0007	-0.08
40	high decorrelation		

All of the tensile tests including tensile test on regular sample, strain concentration test and crack detection tests were done with the same tensile test device as shown in Figure 28. The uncertainty of the strain gauge was 0.0005in. Sample is fixed at one end while displacement was applied to its other end. This is how tension was applies to the samples.

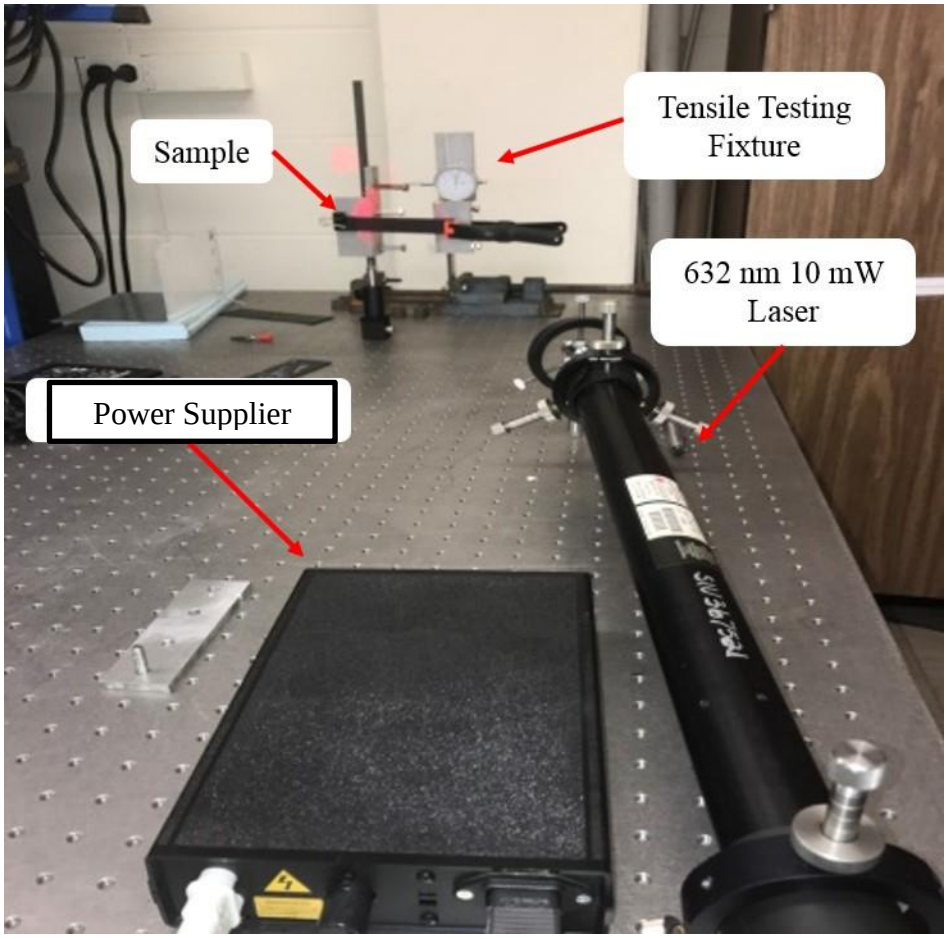

Figure 28: tensile testing setup

CHAPTER 4:

EXPERIMENTS PROCEDURE:

This chapter describes the experimental procedure at each step. First, a translation test was done to evaluate the system's capability in surface displacement measurement. After achieving comparative results in displacement measurement, we evaluated the system performance in strain measurement. This test gave a good outcome for the system's performance in strain mapping and finding strain concentration. Eventually, DiLSIC's capability was examined in finding sub-surface defects. In the last step, DiLSIC was integrated with shearography to show the possible application of this technique in industry.

4.1 Translation Test

The first step of the experiments was the translation test. In this test, the performance of system in surface displacement measurement was evaluated. First an aluminum sheet was translated on the optical table. Aluminum sheet was chosen due to the broad application of metal in industry. In the initial step of this experiment, aluminum sheet with some initial texture on it was used (as can be seen in figure 20). Then the uniform white painted was applied to remove the probability of texture effect on the experimental procedure.

Software reveals the results of displacement in pixel units. Therefore, the pixel size must be found prior to displacement measurement. To measure the pixel size, the image in Figure 29 had to be captured.

Different values of displacements were applied to the samples. The displacement range was [25µm-2540µm]. The applied displacements were in the x direction. The displacement

contours in x direction are being investigated. Uniform color displacement contours are expected due to rigid body displacements.

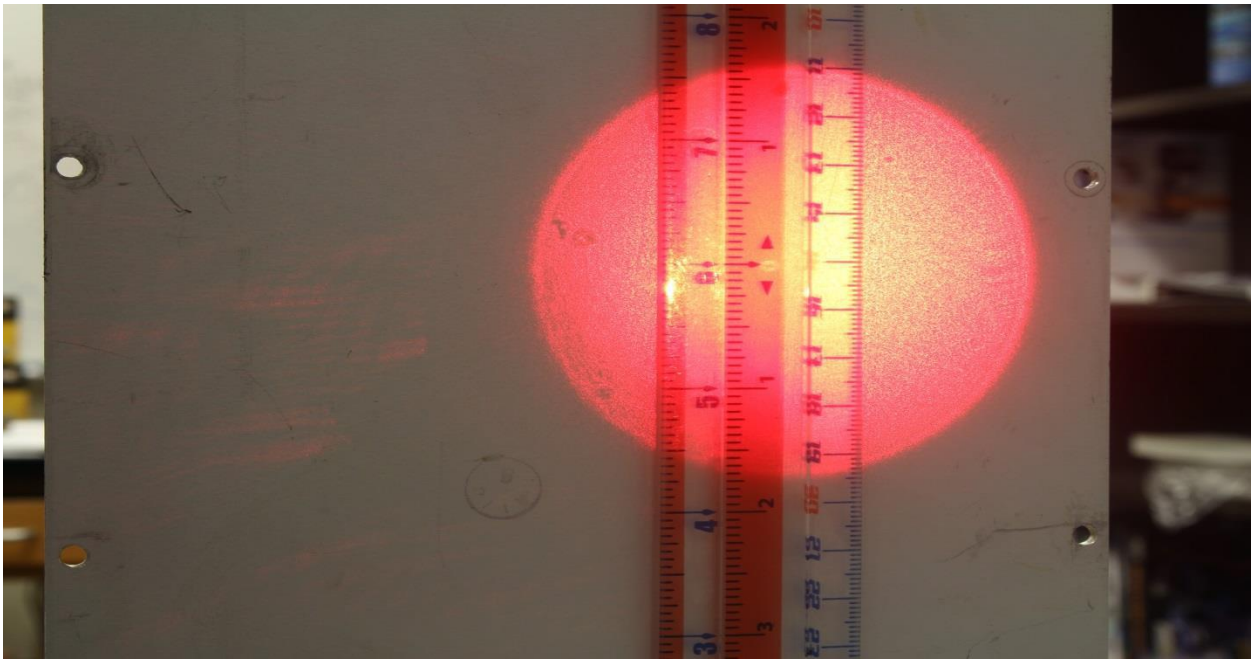

Figure 29: Measuring pixel size by ruler.

In this case, the ruler can show you the real height of your image in relation to the known number of pixels. Therefore, the resulting values given by the software can be converted to metric values.

In the last step of the translation test, rubber was examined since it was going to be used in the rest of the experiments.

4.2 Tensile Test:

After proving the system's capability in measuring displacements of the surfaces, we intended to evaluate the system performance in strain measurement. As it was explained before,

a rubber sample was used in the rest of the procedure. We wanted to see the strain contours in simple cases such as strain contours in a regular, rectangular sample after applying tension.

Tensile tests were done using both DIC and DiLSIC methods for comparison. Different values of tension were applied to the sample in x direction. It is expected that in strain less than 2% DiLSIC will be more accurate due to the use of a laser speckle pattern. Also, since there is no defect or irregularities in the sample geometry, the uniform color strain contour is predicted in both cases (DIC and DiLSIC).

4.3 Strain Concentration Inspection

In this step, the system's performance in detecting strain concentration was evaluated. The previous step showed how the system works in strain measurement. Strain is important, because by finding locations of strain concentration, we will be able to predict the future fracture, investigate the crack propagation, fatigue analysis, etc. After achieving good results of system performance in strain measurement of a regular sample, the capability of system in strain/stress concentration location was investigated. In order to evaluate this fact, a 1cm diameter hole was created in the sample that what was used in the tensile test. This hole caused a strain concentration due to irregularity in geometry.

In this process, same amount of tensile force was applied to the DIC sample and the DiLSIC sample, then the contours were compared. After that, the point with maximum strain was chosen to draw a line through, perpendicular to bottom of the sample. This line shows the broadest range of strain value in this experiment. Later this line was used to quantify the strain concentration comparison. The strain values of a few points along this line in the DiLSIC sample were compared to similar coordinate points in the DIC sample.

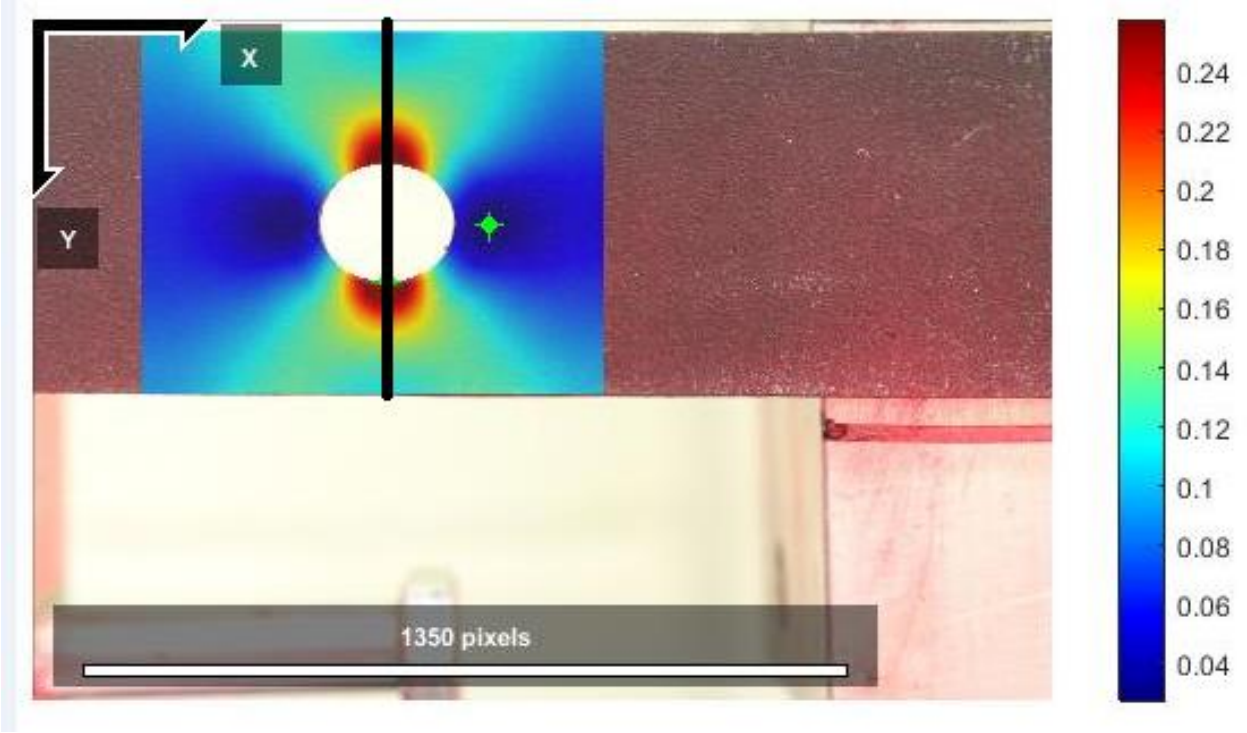

Figure 30: Created Line used to compare the strain value

4.4 Subsurface Crack Detection

In this step the prepared sample was illuminated by the expanded laser beam. Certain values of tension were applied to the sample by the tensile testing device. The minimum tension which would show signs of cracks is selected to be simulated in ANSYS. The FEA contour was compared to the DiLSIC contour to validate the technique. It should be noted that the crack could not be detected through the DIC method; otherwise, results would be compared to DIC results.

4.5 Shearography Integration

In the Digital Laser Speckle Image Correlation (DiLSIC) method, an expanded laser beam is projected to the target surface. The created laser speckle patterns are used to track

deformation with the digital image correlation method. DiLSIC was used for strain mapping with LTI-2100.

In the first step, translation was done on the sample. The capability of the system in recognizing and estimating the displacement values led us to identify and measure the strain due to a regular tensile test in the second step. After finding good results in the tensile test step, stress concentration was investigated in the last step. Results of the translation and tensile tests were compared to their actual values while the resulting strain concentration contours were compared to their DIC counterpart. In the other words, all of the processes done to validate DiLSIC, were repeated after integrating with the shearography device. Images captured by the shearography camera were incorporated into the DIC methods. First the lasers of LTI-2100 were used to illuminate the samples. In later steps, the described laser was used for illuminating the samples while images were captured by the shearography camera.

CHAPTER 5

RESULTS AND DISCUSSION

In this chapter, results of each experiment is presented and discussed.

5.1 Translation Results

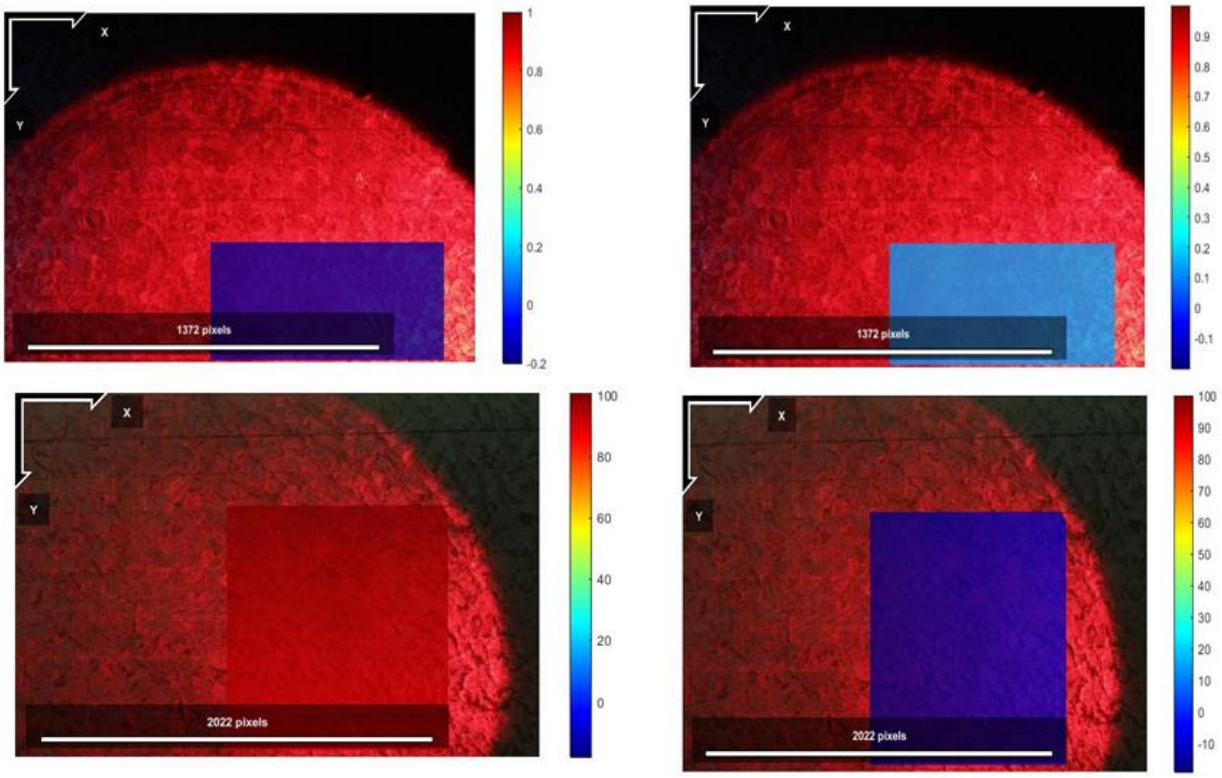

Figure 31: Displacement contours in x direction.

Figure 31 depicts the displacement contours in x direction which was the direction of applied displacement. As it was expected, we have uniform color displacement contours due to rigid body displacements. As can be seen in Figure 31, the sample has some texture itself. In order to eliminate the influence of texture instead of laser speckle patterns, similar sample with the uniform white paint on it was tested as well.

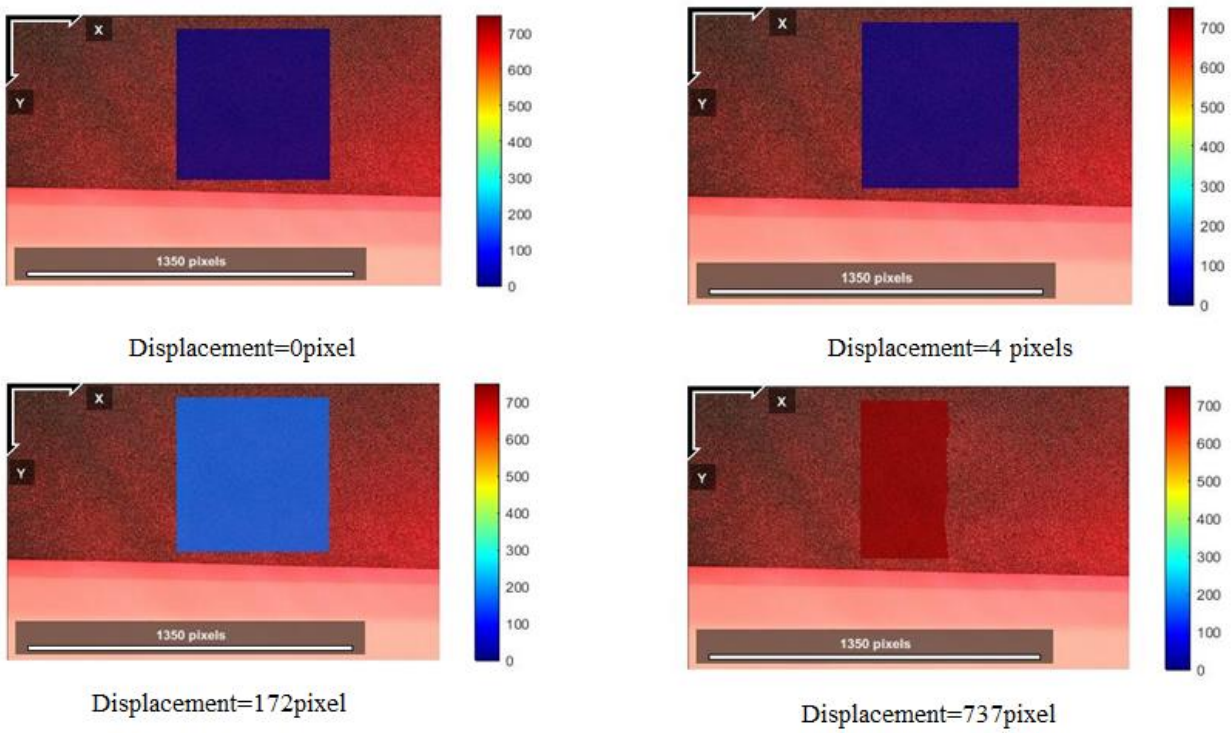

Figure 32: displacement contours in x direction-rubber sample

From the resulted displacement contours, it can be concluded that, texture of the surfaces are not the mean to track displacement for DiLSIC, but it is able to map and measure displacement by using laser speckle pattern. Now in the following tables and figures, we are going to quantify this comparison.

Table 4: Actual displacement vs DiLSIC measured displacement- White painted

Actual displacement	displacement (pixels)	displacement (µm)	error
50	0.8527	47	0.044976
75	1.3361	74	0.002379
100	1.6827	94	0.057688
150	2.624	146	0.020373
175	3.0955	173	0.00944
200	3.5305	197	0.01146
225	3.9589	221	0.014674
300	5.3989	302	0.007795
325	5.7607	322	0.007387
350	6.2586	350	0.001376
375	6.7107	375	0.002131
400	7.1347	399	0.001142
425	7.5685	423	0.002739
475	8.4896	475	0.000879
500	9.0365	506	0.012088
525	9.3645	524	0.00112
550	9.7779	547	0.004432
575	10.1909	570	0.007495
600	10.64484	596	0.006482

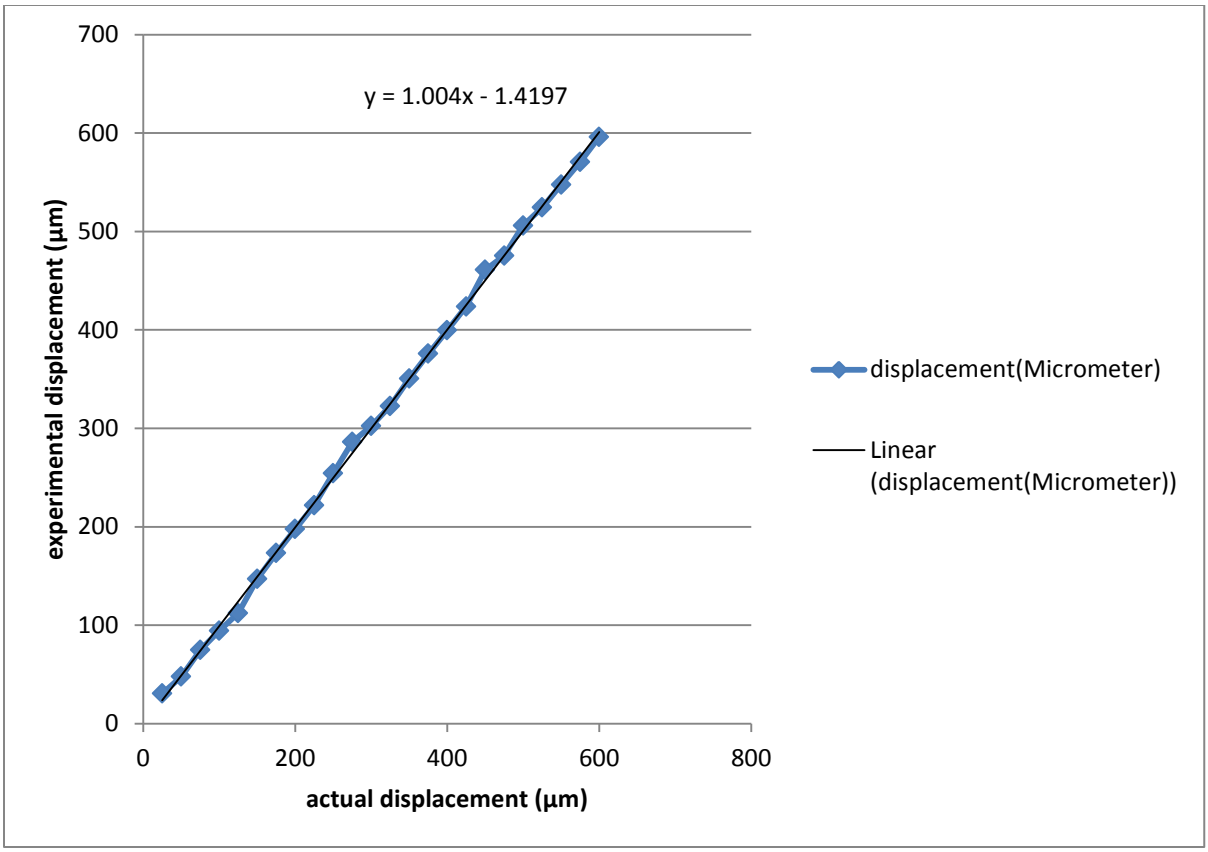

Figure 33: Actual displacement is x direction vs the measured displacement by DiLSIC-white painted Aluminum

It is worth noting that, with this hybrid method we were able to measure displacement from 25µm to 2540µm, which was a very good achievement. The slop of the line shows the well agreement between actual and DiLSIC measured displacement. The average error was 0.4% which is another magnificent achievement. It should be reminded that traditional DIC was not able to measure displacement in micro size with regular digital camera. Also based on the Phys work, measuring displacement more than 1mm was not possible while using laser DIC could broad the range of measure displacement to 1in. figure 34 and table 5, compare the measured displacement with DiLSIC and actual applied displacement in x direction of rubber material.

Table 5: actual displacement vs DiLSIC measured displacement –rubber

Actual (in)	U(Pixel)	U(in)	error%
0	-0.237	-0.00031	
0.005	4.12	0.0053	6
0.2	171.81	0.2233	11.67
0.9	736.94	0.958	6.44
Actual (in)	U(Pixel)	U(in)	error%
0	-0.237	-0.00031	
0.005	4.12	0.0053	6
0.2	171.81	0.2233	11.67
0.9	736.94	0.958	6.44

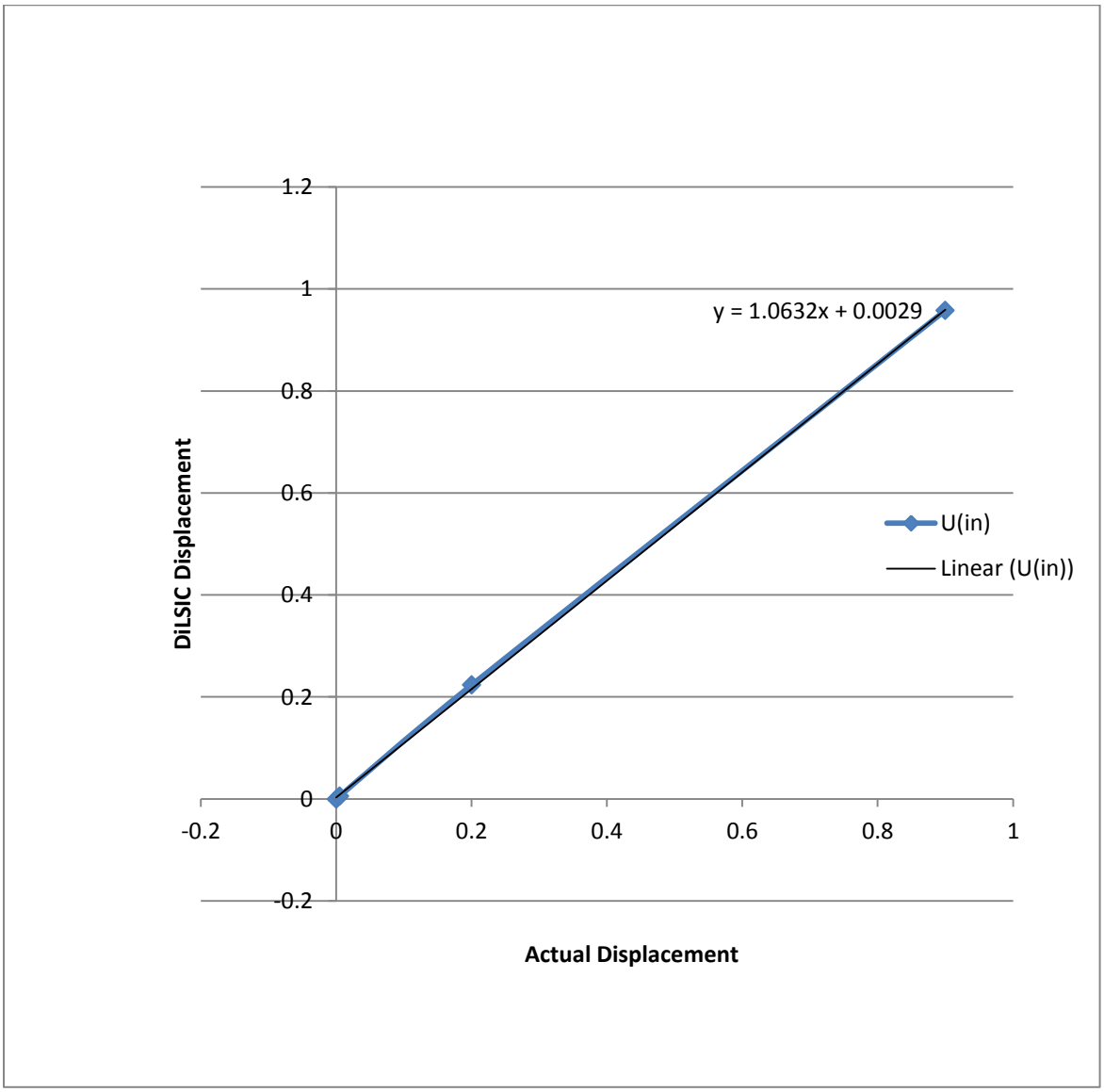

Figure 34: comparison between measured DiLSIC displacement and actual displacement of rubber

5.2 Strain Measurement Results

In figure 35, the contours of strain in both methods can be compared. The same values of strain were applied in both cases in this figure. High agreement between contours is the first step to show the DiLSIC precision in strain mapping.

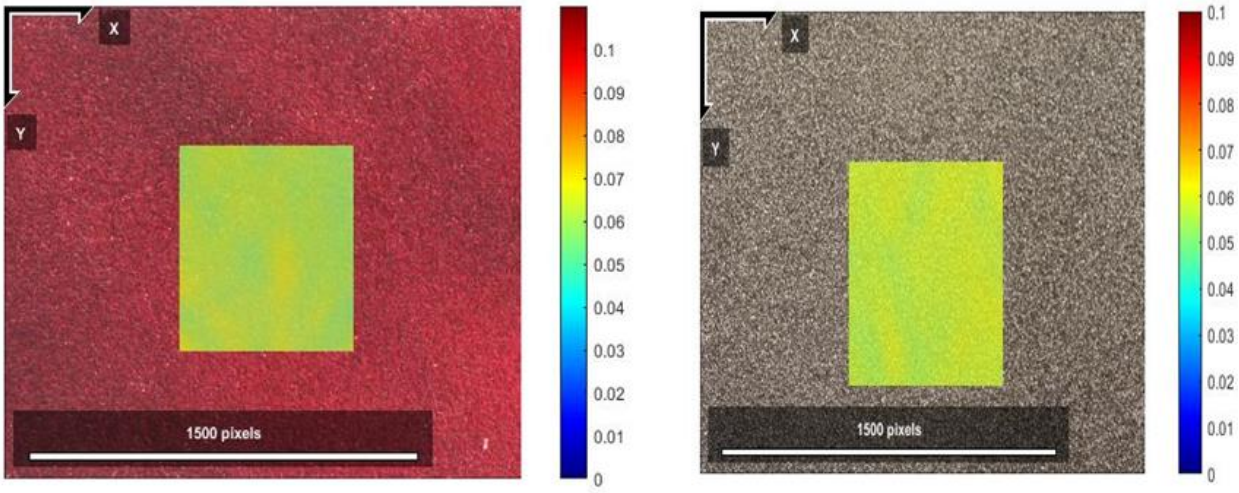

Figure 35: strain contours in x direction. DiLSIC contour (left), DIC contour (right)

Table 6 quantifies the comparison between methods. As can be concluded from the table, DiLSIC results in strain, lower than 2% is more comparative than DIC which was predicted. As it was discussed before, laser speckle is one of the best choices for measuring small displacement and strain. Laser speckle sizes did not exceed 1µm. this fact gives us the ability to measure the displacements and strain in micro size without using a microscopic camera. In table 6, the results of tensile tests in regular rectangular sample can be compared.

The RG-DIC radius adjusted as 29. Strain radius and subset spacing were adjusted as 15 and 2 respectively.

Table 6: Actual Strain vs DIC and DiLSIC measured strain

actual displacement	actual strain	Dilsic strain	Dic strain	dilsic error %	dic error %
0.05	0.01	0.011	0.0084	10	16
0.08	0.016	0.017	0.0139	6.25	13.12
0.1	0.02	0.0209	0.0179	4.5	10.5
0.12	0.024	0.0245	0.0218	2.08	9
0.15	0.03	0.0302	0.0277	0.6	7
0.2	0.04	0.0404	0.0379	1	5.25
0.25	0.05	0.05	0.0482	0	3.6
0.3	0.06	0.0602	0.0586	0.3	2
0.35	0.07	0.0698	0.069	0.28	1.4
0.4	0.08	0.0797	0.0795	0.375	0.62
0.45	0.09	0.0893	0.09	0.78	0
0.5	0.1	0.0994	0.1006	0.6	-0.6

As can be understood from the table 6, DiLSIC did a very good job in strain lower than 2%. The other notable conclusion is that DiLSIC is as good as traditional DIC in measuring strain more than 2%.

Figure 36, shows the comparison between DIC and DiLSIC in strain measurement. All of the results were compared to the actual strain values.

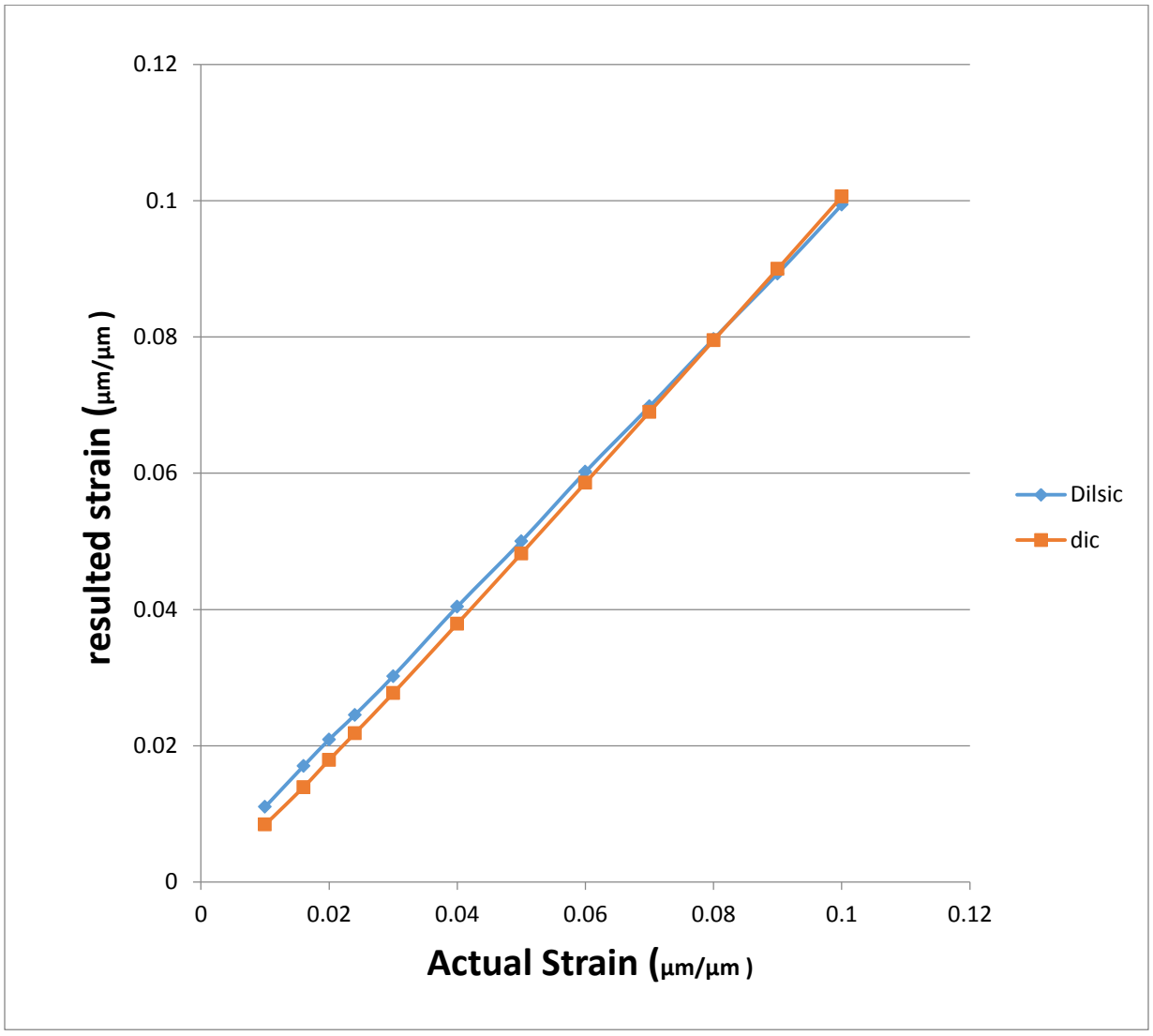

Figure 36: DiLSIC and DIC measured strain in compare to actual strain

Again as it is shown in figure 36, the strain values of DiLSIC are closer to the actual strain values in smaller range strains while in larger strain the results of DiLSIC and DIC are close to each other.

5.3 Strain concentration detection

In figure 38, the high agreement between contours of strain in DIC and DiLSIC, is the evidence of DiLSIC great potential in detecting stress/strain concentration. The green points shoe the location of maximum and minimum strain.

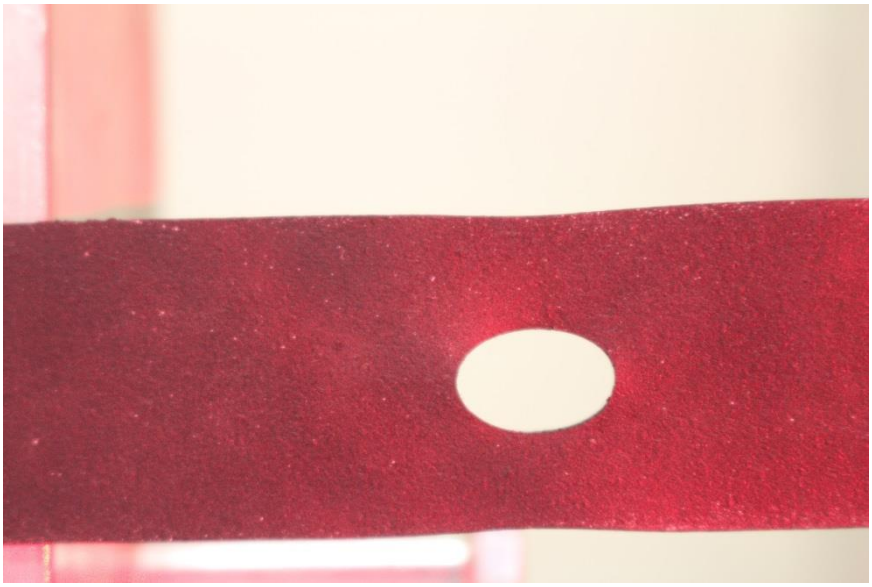

Figure 37: sample used for strain concentration monitoring after deformation.

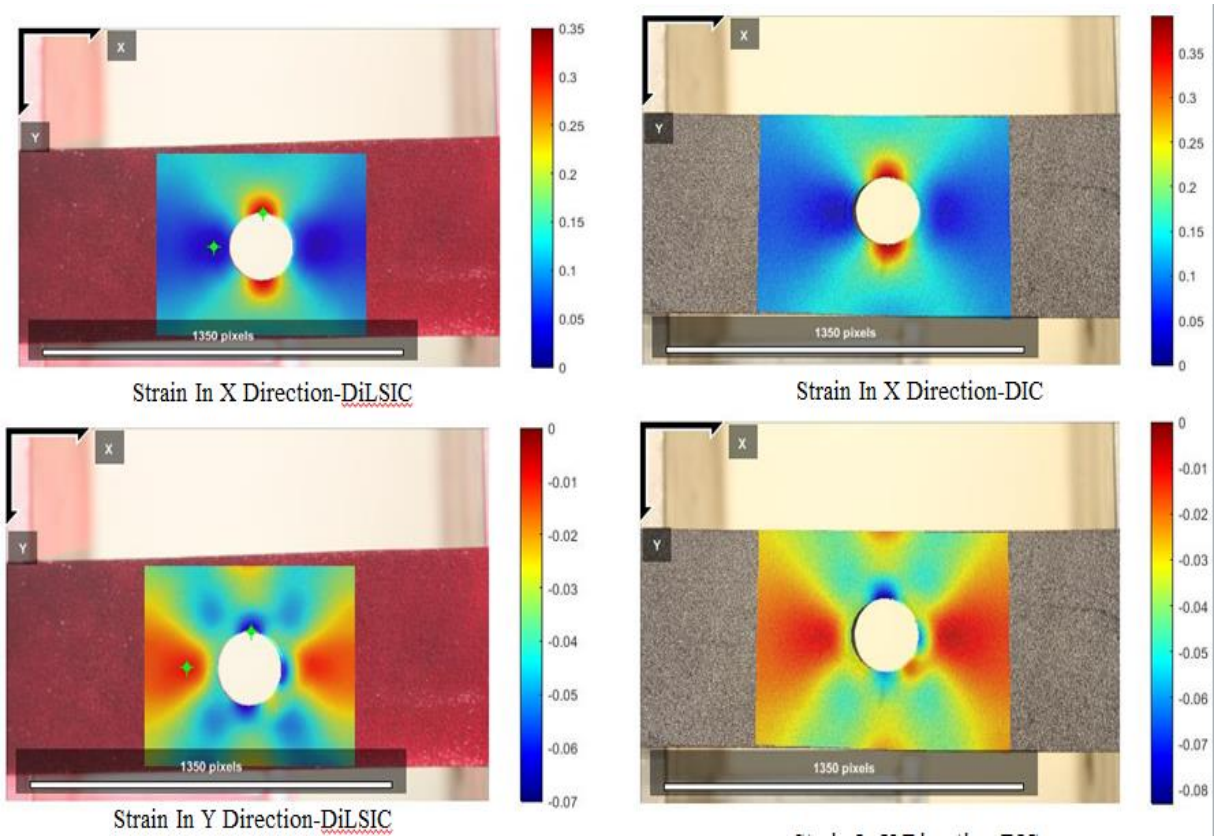

Figure 38: Strain contours comparison in case of having strain concentration in both DIC and DiLSIC

As it was explained, an imaginary line created to quantify the comparison. A few points were selected along this line and the values of the strain of those point were compared to the values of strain of similar points in DIC samples. The comparison can be found in figure 39.

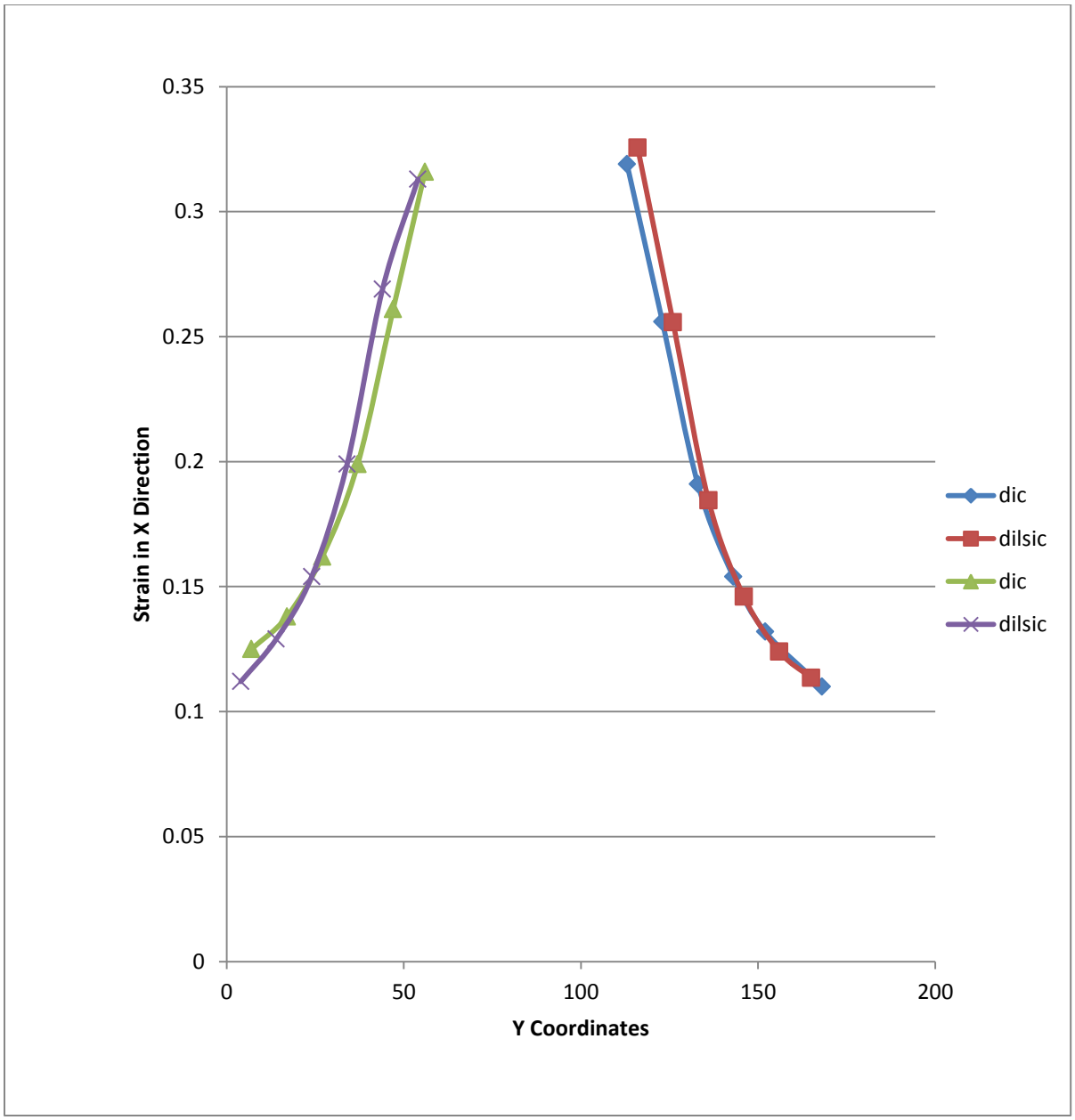

Figure 39: quantified comparison between DiLSIC and DIC in strain mapping.

5.4 Crack Detection Results

The results from the last experiment are depicted in Figure 40. The contours show the system's performance in finding non-surface cracks. Based on the obtained results, the sub-surface crack can be located by DiLSIC which has a great potential to be followed as the further researches. As can be found in figure 40, the sub-surface crack location is in between the two connected area with the higher strain rate. The determined points in figure 40, marked the maximum and minimum strain location. The agreement between contour of simulated FEA model and DiLSIC validates this method.

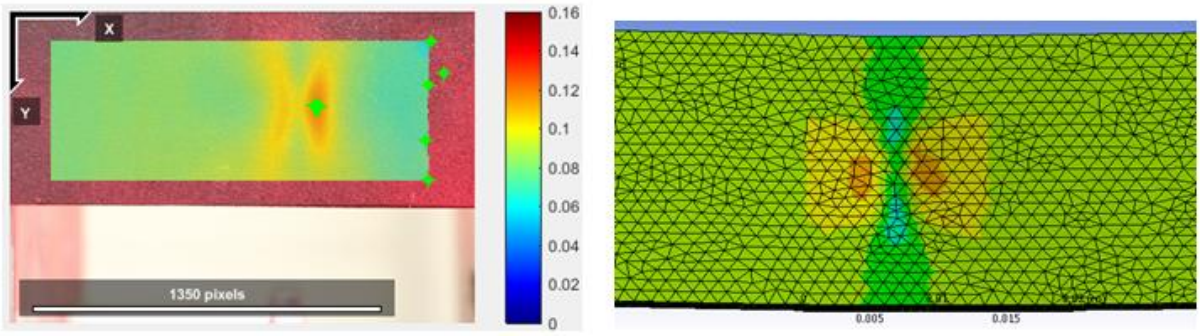

Figure 40: Strain contours in x direction used for sub-surface crack detection contours. DiLSIC contour (left), FEA simulation of crack area (right)

5.5 Integration with Shearography Results

As it was described in the procedure part, all of the tests and experiments done to validate DiLSIC, were repeated to validate this integration. Tests including translation, tensile test on the regular sample, strain concentration detection was with the shearography device. In the following figures the results of this integration can be found.

5.5.1 Shearography translation test results

Table 7: translation test quantified results

Displacement actual(µm)	Displacement calculated(pixel)	Displacement Calculated(µm)	Error %
279	2.78	261	6
1270	14.9	1402	10
2540	27.98	2634	3.7
3302	35.24	3317	4.7
5080	54.25	5107	0.5
7620	82.28	7746	1.6

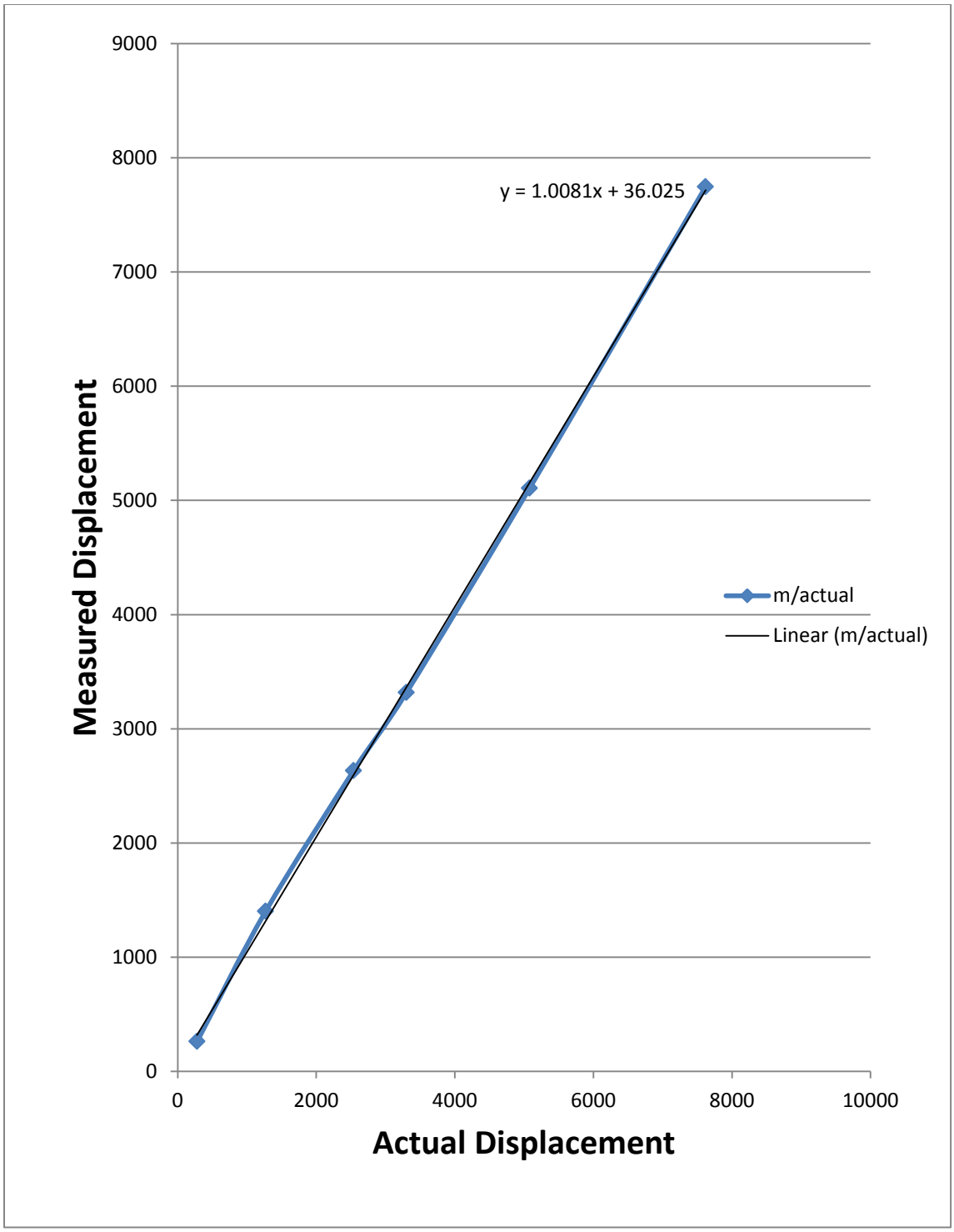

Figure 41: Calculated displacement vs Actual displacement Results

The slop of the line in figure 41, shows the well agreements between the actual displacement and measured displacement with shearography device. Also the average error is about 0.8% in displacement measurement which declares a good achievement in the first step of integration evaluation. Capability of system in displacement measurement was proved in this test, therefore we were led to the next step of evaluation.

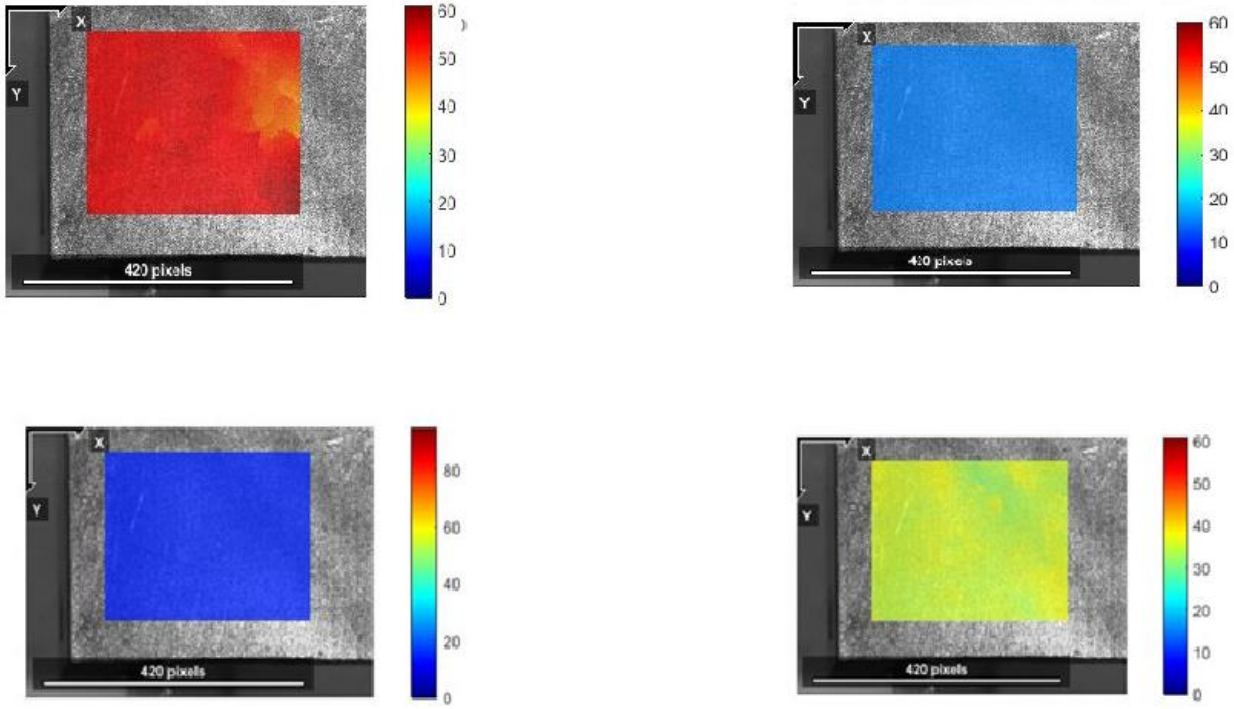

Figure 42: Translation Test results-Displacement contours in x directions

Uniform displacement contours were expected due to rigid body motion. Displacement was applied in x direction.

5.5.2 Tensile Test on the regular sample results of integration

Table 8: comparison between DiLSIC, Integrated system and DIC in strain measurement

actual displacement	actual strain	DiLSIC strain	DIC strain	Shearography strain	DiLSIC error	shearography error	DIC error
0.05	0.01	0.011	0.0084	0.0109	10	9	16
0.08	0.016	0.017	0.0139	0.016	6.25	0	13.125
0.1	0.02	0.0209	0.0179	0.0197	4.5	1.5	10.5
0.12	0.024	0.0245	0.0218	0.0234	2.08	2.5	9.1
0.15	0.03	0.0302	0.0277	0.0302	0.67	0.67	7.6
0.2	0.04	0.0404	0.0379	0.0398	1	0.5	5.25
0.25	0.05	0.05	0.0482	0.0499	0	0.2	3.6
0.3	0.06	0.0602	0.0586	0.0608	0.34	1.3	2.3
0.35	0.07	0.0698	0.069	0.071	0.28	1.43	1.4
0.4	0.08	0.0797	0.0795	0.0816	0.375	2	0.625
0.45	0.09	0.0893	0.09	0.0925	0.78	2.7	0
0.5	0.1	0.0994	0.1006	0.1077	0.6	7.7	0.6

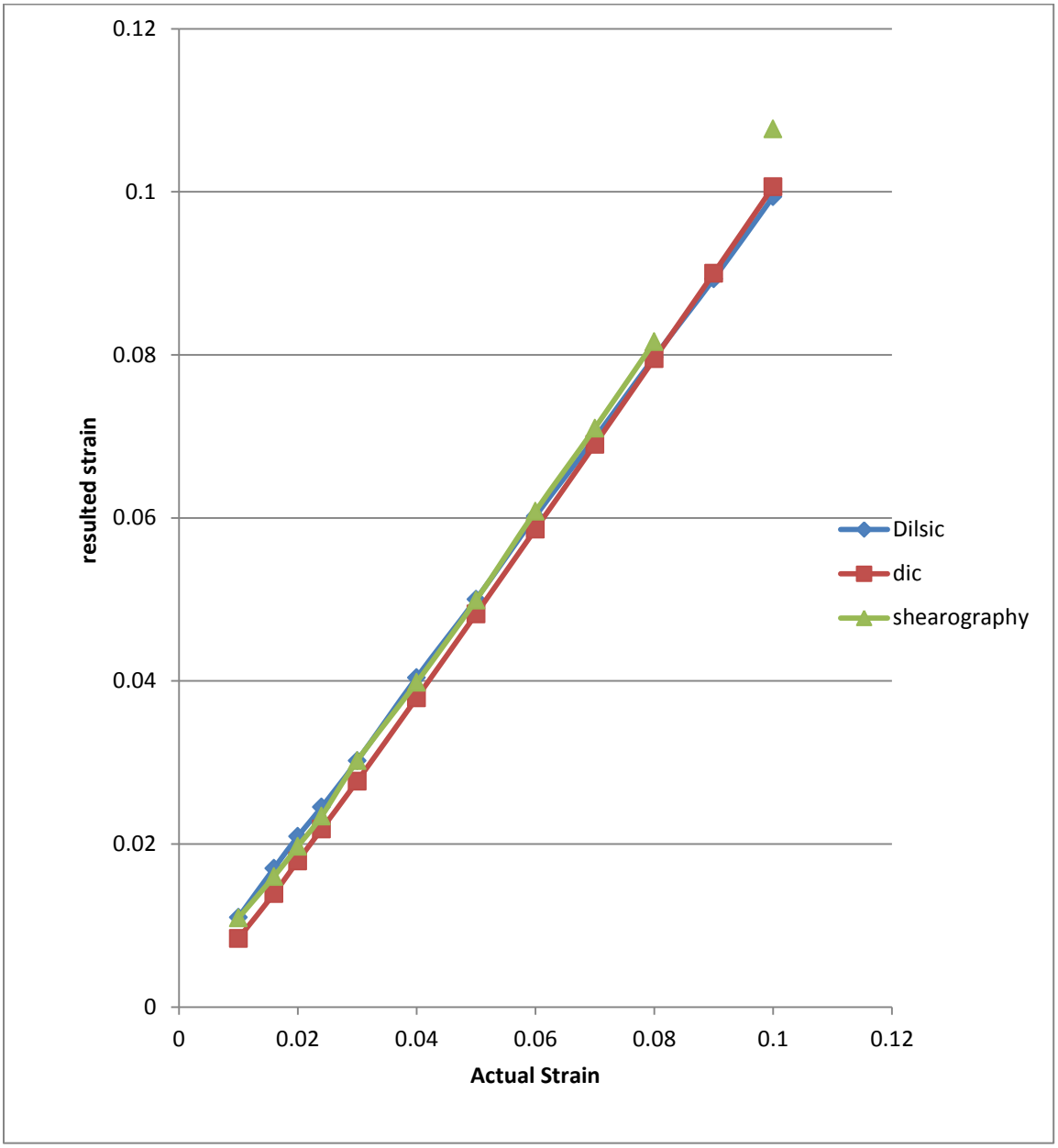

Figure 43: comparison between DiLSIC, Integrated system and DIC in strain measurement

Comparison between actual strain and measured strain with laser speckle and shearography camera, shows the capability of integrated system in finding strain. Sample used in this test is

shown in figure 1. It had no defects or any geometry which can cause strain concentration. Therefore, the uniform strain contour was expected. Strain contours are shown in below.

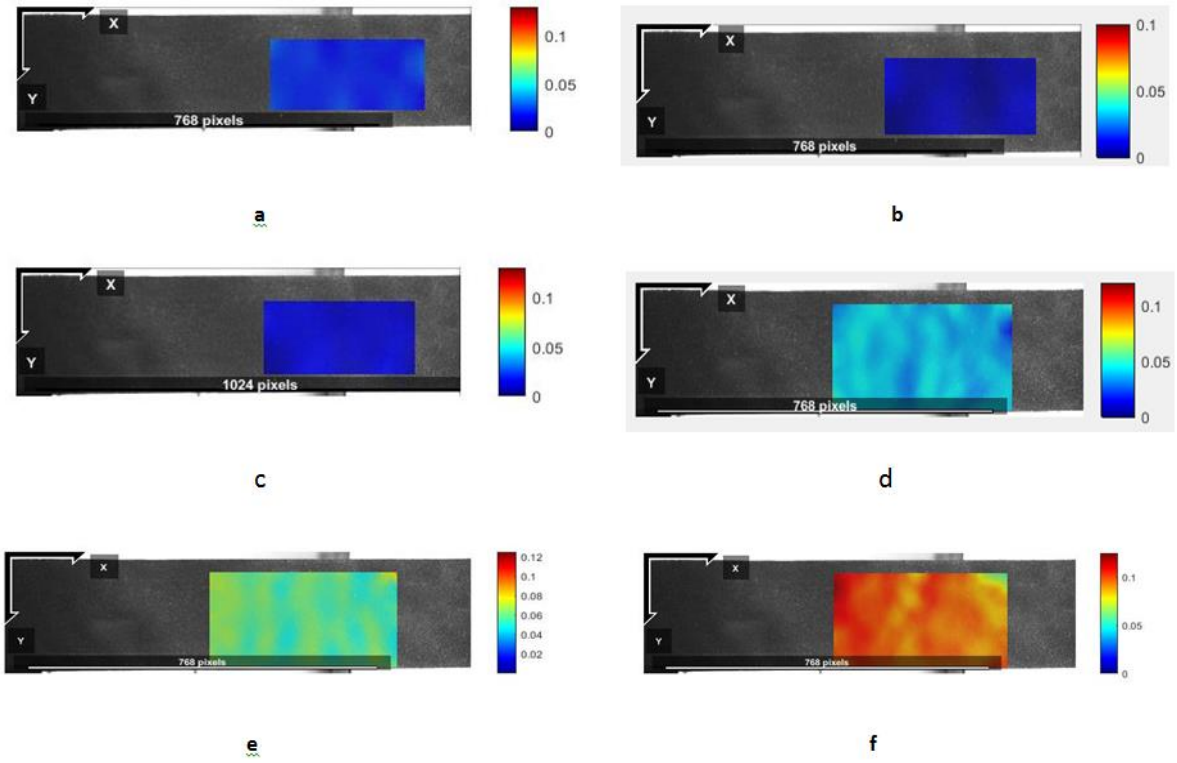

Figure 44: Strain Contours. Actual strain in each case was (a):0.02-(b):0.0005-(c):0.012-(d):0.04-(e):0.06-(f):0.12

5.5.3 Strain Concentration

The red areas can shoe the strain/stress concentration in both contours. This integration can lead to predict the location of future fracture. The high agreement between strain contours in DIC and Shearography/ DiLSIC integration, prove the feasibility and capability of it.

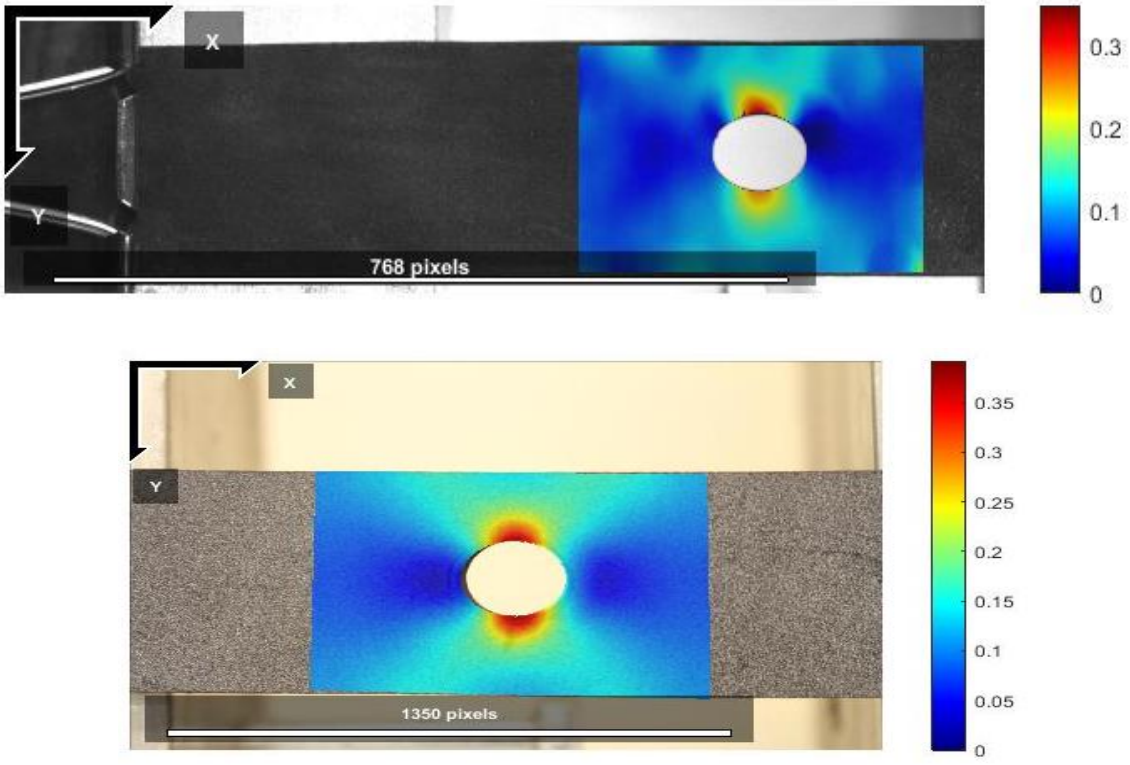

Figure 45: comparison between DIC and Shearography camera in strain concentration contour

5.5.4 Integration Discussion

Current used images resolution could not exceed 1024×1024. This feature made it difficult to track the sub images by Ncorr. Also moving shearography lasers to the back of camera in order to provide more distance between the target surface and expanding lens will

make them useful for strain mapping as well as defect detection. Since the speckle size is found by equation 6, which has the direct relationship with distance between expanding lens and target area, while the camera should be located close to the target surface. λ shows the wavelength, Б is the speckle size, q is distance between lens and target surface and D is the aperture size.

$$Б=1.2\times q\lambda/D \tag{6}$$

CHAPTER 6

CONCLUSIONS AND RECOMMENDATIONS

In the first step of experiments, system capability in tracking surface displacement was evaluated. The displacement in range of [25µ-2540µ] which was a great achievement because it could exceed the laser interferometry based methods measurement (1mm) . Also it could compensate DIC error in micro-size displacement measurement due to using smaller speckle size. It is worth noting that micro-size displacement measurement was achieved by using regular digital camera instead of microscopic cameras. Evidence of system precision in displacement measurement led us to evaluate DiLSIC performance in strain mapping. Results of tensile test on regular sample validate this method as the good alternative for laser based methods such as ESPI and DIC in strain mapping.. crack detection experiment proved the capability of this hybrid method in sub-surface defect detection which is a significant achievement in NDT optical method. This method could broaden the application of optical NDT techniques by not using artifact speckle pattern (such as spray painting). Also micro size laser speckles allow us to measure micro size displacement with a regular digital camera.

Perfect results in strain mapping of the sample with strain concentration showed DiLSIC potential in strain mapping of objects with complicated geometry. Also using DIC in this combination allow user to inspect objects under complicated loading, such as buckling.

These results validated the integration of Shearography device with DiLSIC method for strain mapping. This integration can help us with fracture prediction and locating stress

concentration. Increasing the saved images resolution can be very helpful. This integration can be done by making four changes in the current system:1) increasing shearography camera resolution; 2) adding an auto-set system to focus the camera automatically on the target surface and shearography set to remove the duplicated image out of ROI; 3) adding the appropriate code to shearography current software to do image processing based on DIC method; and 4) setting a new laser in the maximum distance from the shearography camera to create the largest laser speckle pattern on the target surface.

APENDICES

Appendix A: CAMERA SETUP

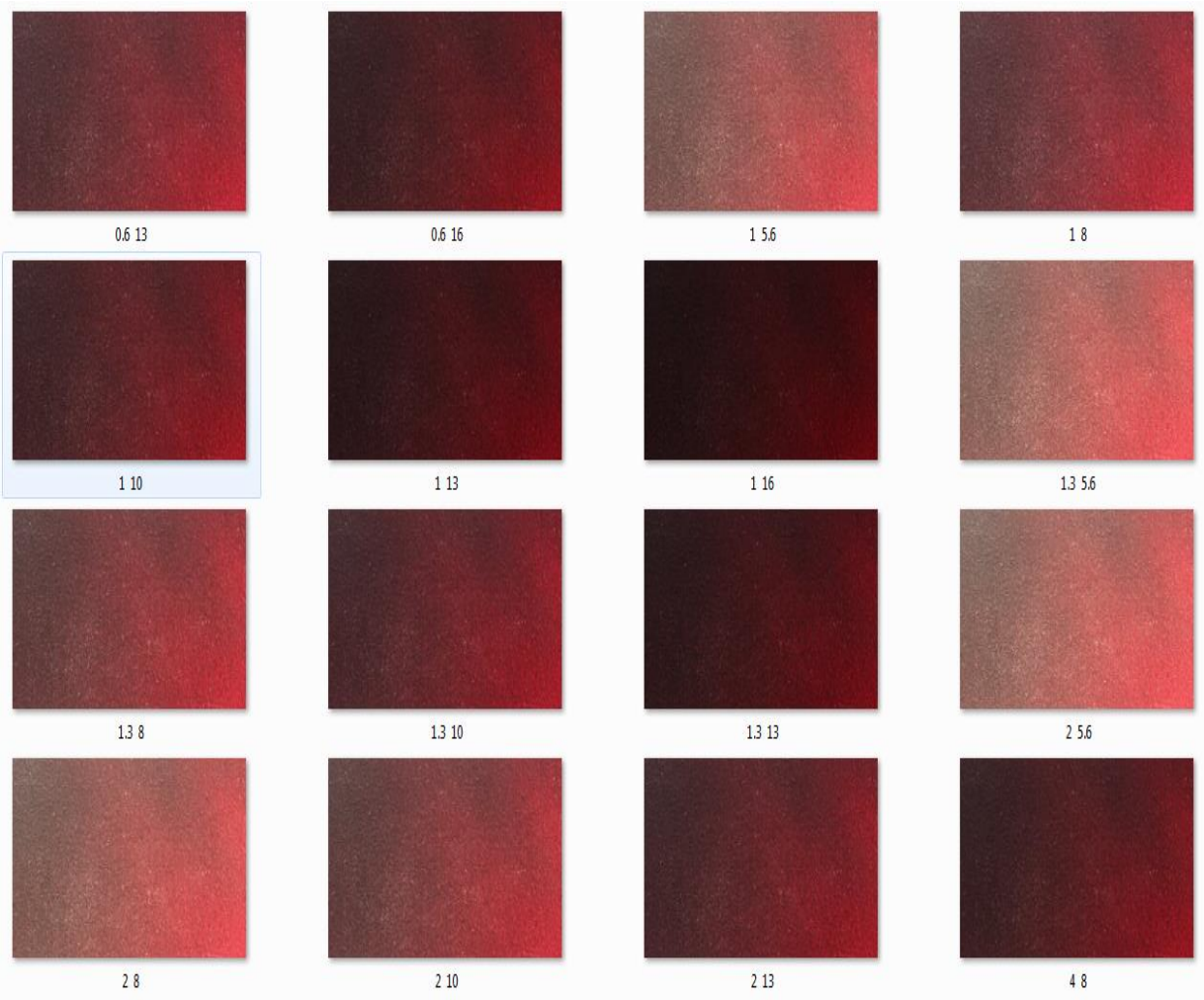

Figure 46: different camera setup. Number in left showes the time of exposure and the number in right showes the apartuure size

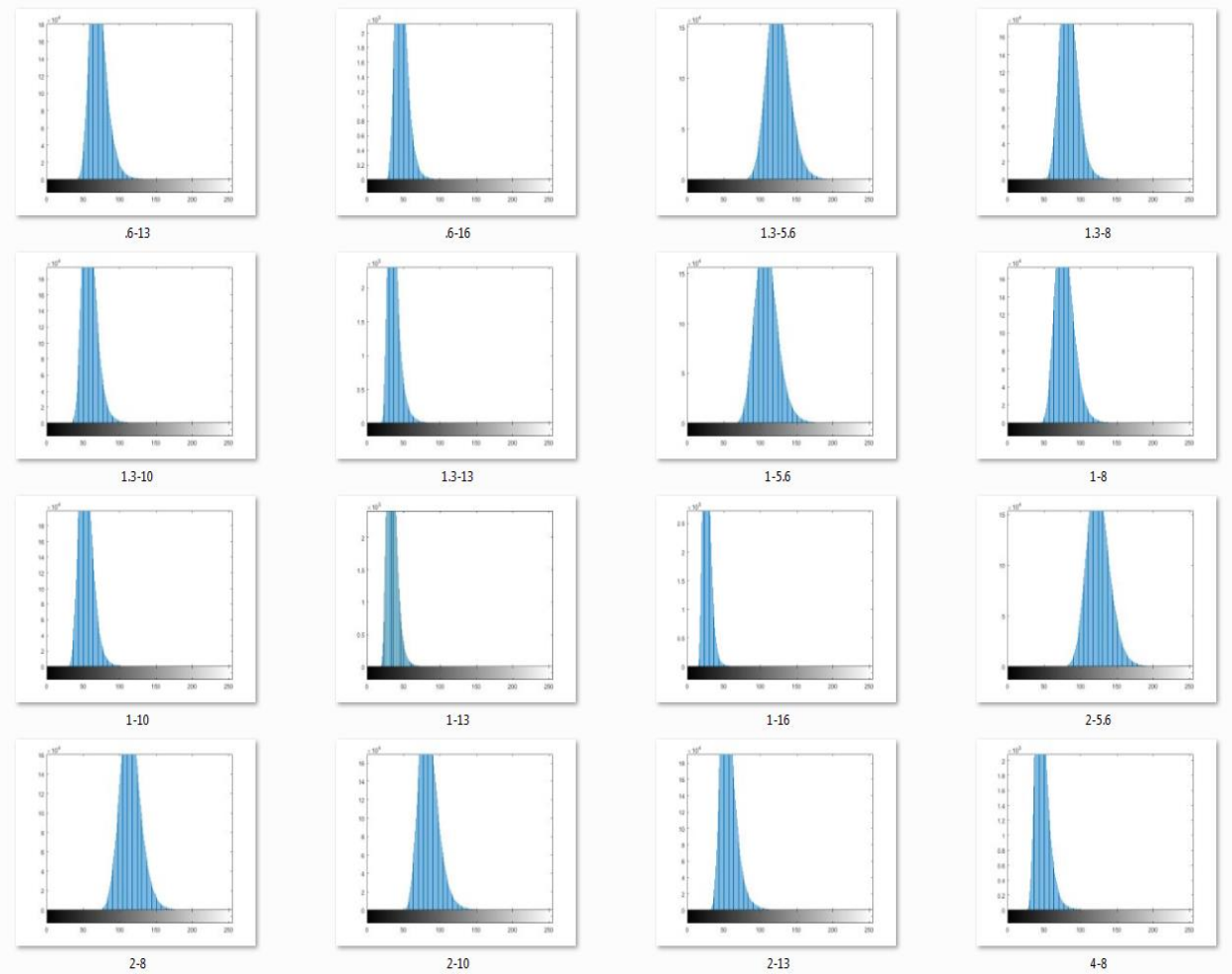

Figure 47: Histogram of images in figure 45

Appendix B: shearing strain and strain in Y direction contours

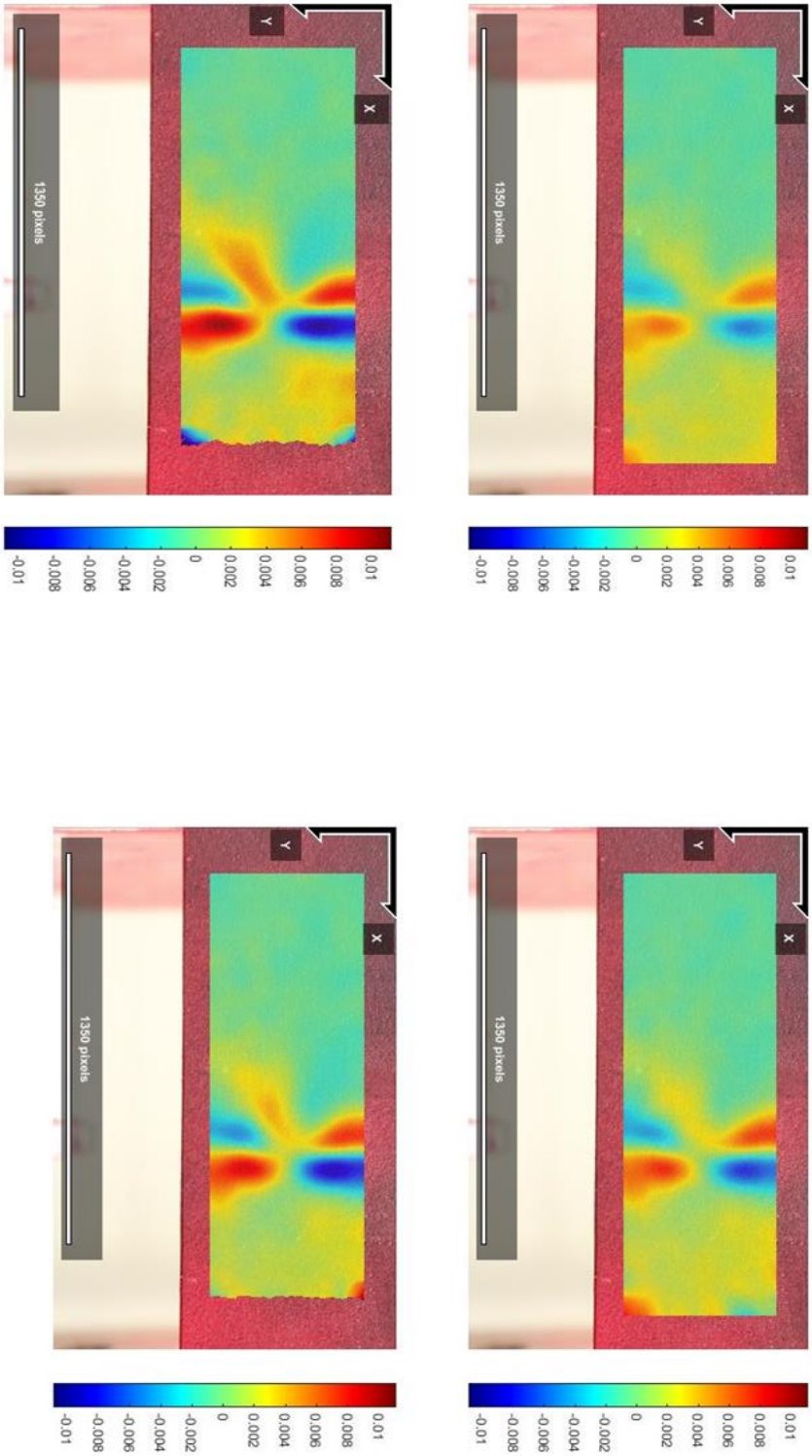

Figure 48: strain in xy plain (shear strain) in sample with sub-surface crack

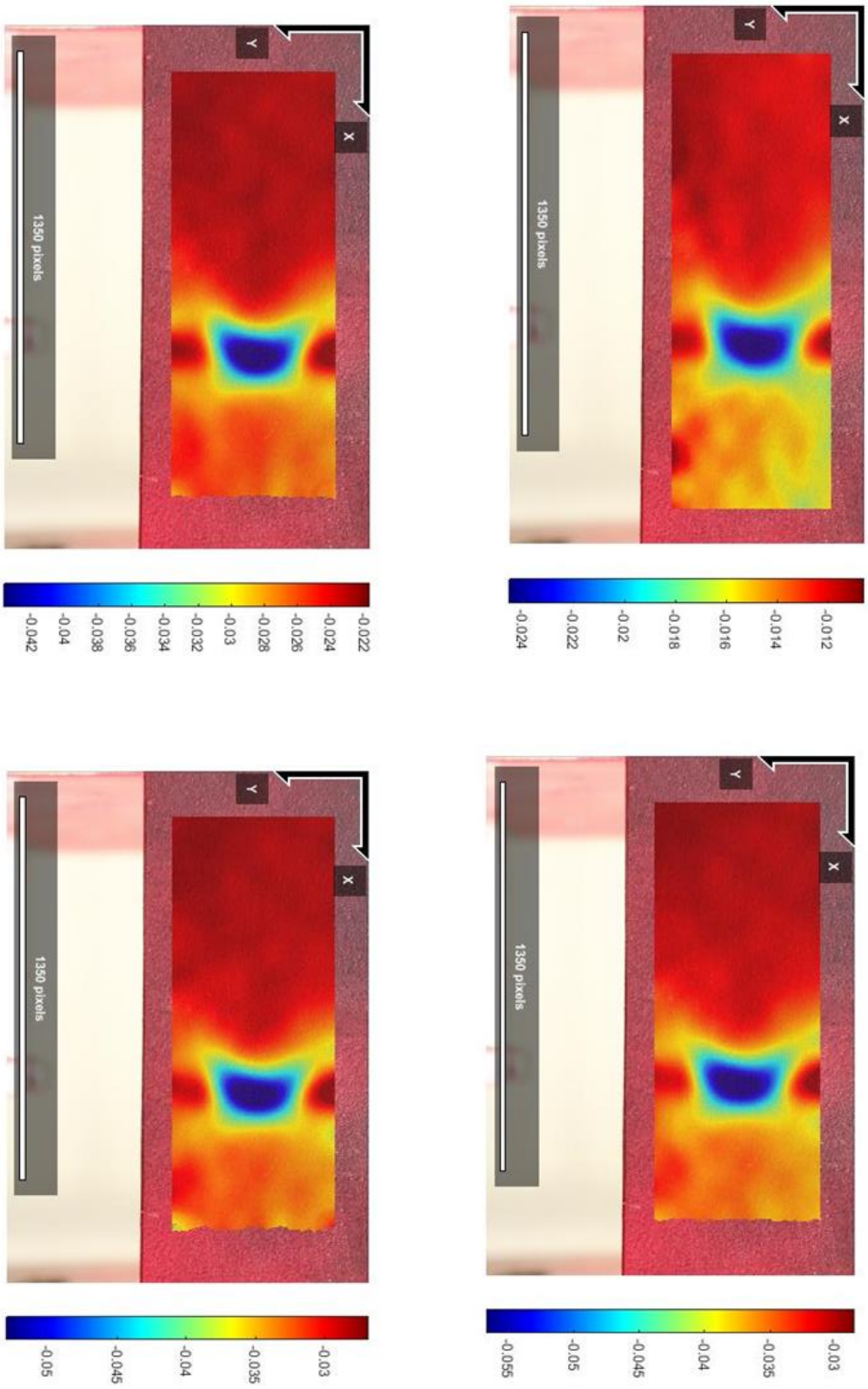

Figure 49: strain in y direction in sample with subsurface crack

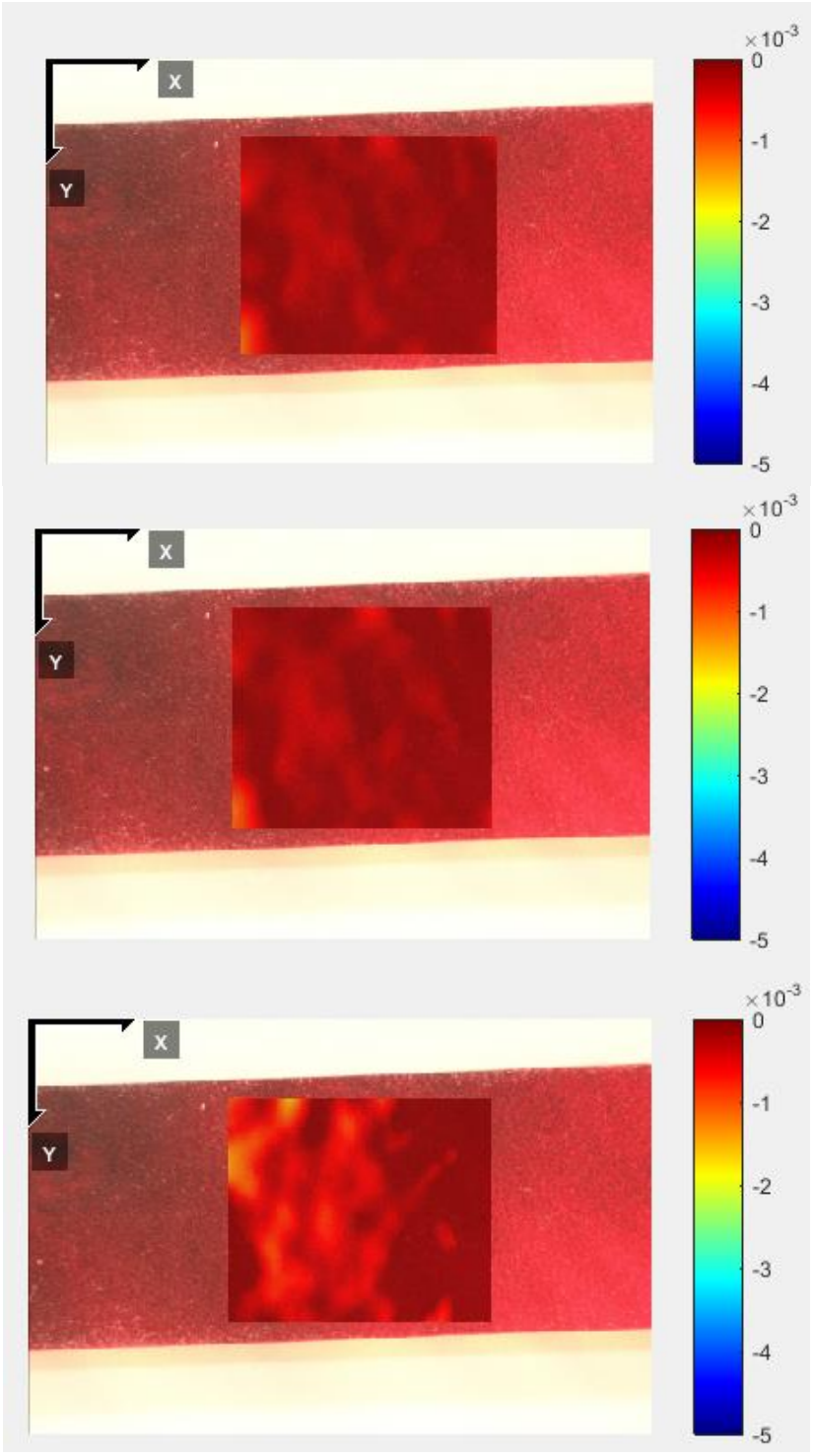

Figure 50: strain contours in y direction in regular rectangular sample

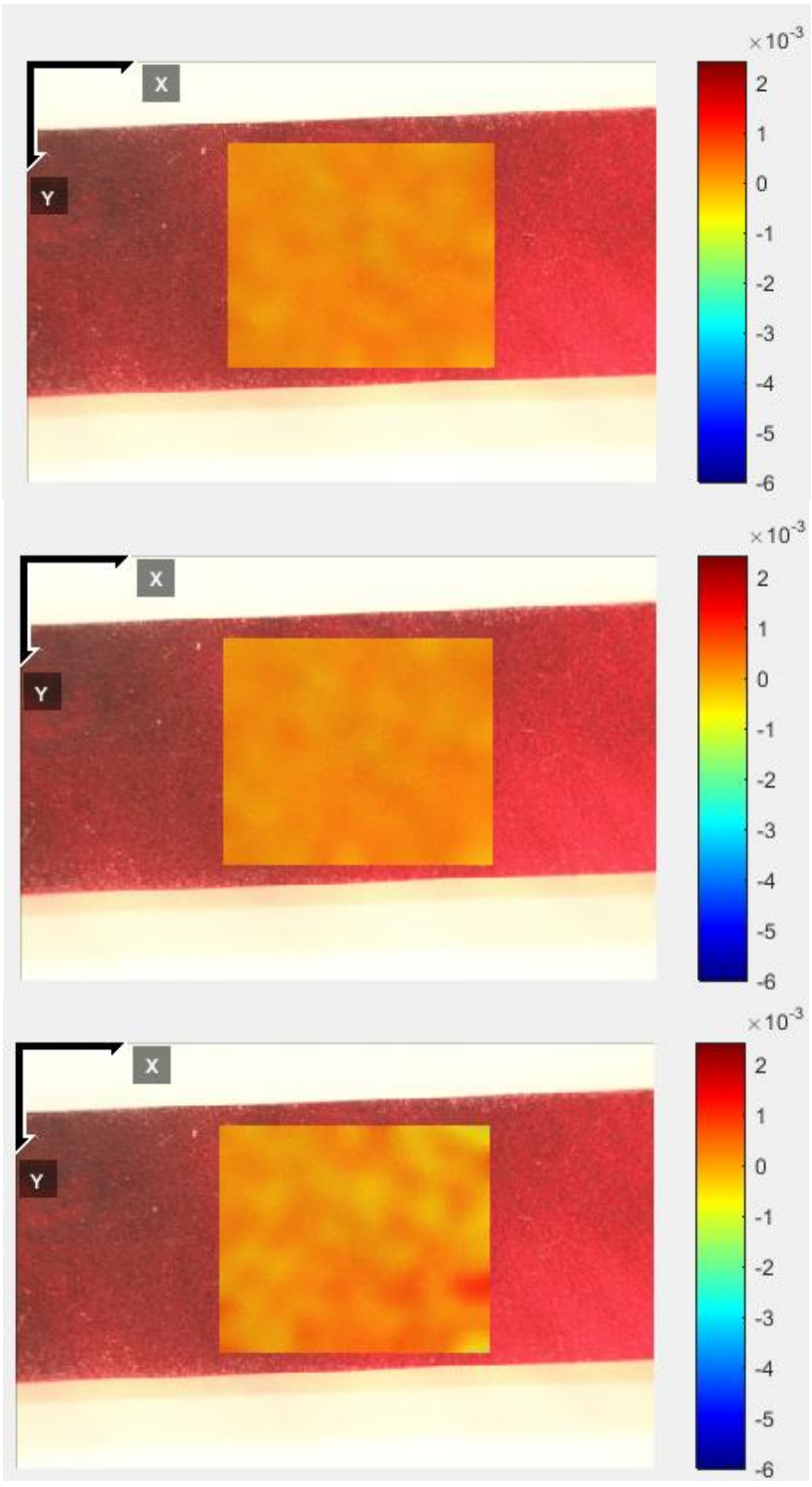

Figure 51: Strain contour in xy plane. Regular rectangular sample in tensile test

Appendix C: Matlab Codes

Code for Average Image:

```
I0 = imread('IMG_0891.jpg');
sumImage = double(I0);
% Inialize to first image.
for i=892:899
    % Read in remaining images.
    rgbImage = imread(['IMG_0',num2str(i),'.jpg']);
    sumImage = sumImage + double(rgbImage);
end;
meanImage = sumImage / 1000;
image(meanImage);
clc;
```

Code for Images Histogram:

```
I=imread('crack_40.jpg');
I=rgb2gray(I);
figure;
imhist(I);
```

REFERENCES:

[1]. T. C. Chu, W. F. Ranson, M. A. Sutton and W. H. Peters, " Application of Digital Image Correlation Techniques to Experimental Mechanics,," Experimental Mechanics, vol. 3, no. 25, pp. 232-244, 1985.

[2]. T. Chu, A. Mahajan and C. T. Liu, "An Economical Vision-Based Method to Obtain Whole-Field Deformation Profiles,," Experimental Techniques, vol. 6, no. 26, pp. 25-28, 2002.

[3]. J .L. W. Carter, Michael. D. Uchic, Michael J. Mills," Impact of Speckle Pattern Parameters on DIC Strain Resolution Calculated from in-situ SEM experiments", The Ohio State University, Columbos, OH

[4]. T. A. Berfield, J. K. Patel, R. G. Shimmin and etc, 2007, "Micro and Nanoscale measurement of Surface and Internal Plane via Digital Image Correlation", Society for experimental Mechanics

[5]. Y. Su, X. Xu and Q. Zhang , 2016"Quality assessment of speckle patterns for DIC by consideration of both systematic errors and random errors", Optics and Lasers in Engineering, University of science and Technology, China

[6]. S. Yoshida,Muchair, I. Muhamad, R. Widiastuti and A. Kusnowo, " Optical Interferometric technique for deformation Analysis", Research and development center for applied physics, Serpong, Indonasia

[7]. J. Perie, S. Calloch, C. Cluzel and F. Hild,2002," Analysis of a Multiaxial Test on a C/C Composite by Using Digital Image Correlation and a Damage Model", Vol 42, No 3. Universite Paris 6, Cedex, France.

[8]. F. Laurin, J.-s. Charrier, D. Leveque, J.-F. Mair, A. Mavel, P. Nunez,2012, " Determination of the properties of composite materials thanks to digital image correlation measurements", Procedia IUTAM 4 , Cedex, France

[9]. J. Tyson and T. Schmidt, Optical Deformation & Strain Measurement in Biomechanics, GOM mbH

[10]. J. Gryagoridis, 212, "Laser Based Nondestructive Inspection Technique" , Springer Science+ Business Media, LLC, Department of Mechanical Engineering, Cape Peninsula University of Technology, Cape Town, South Africa

[11]. J. Brillaud and F. Lagattu,2002, "Limits and Possibilities of Laser Speckle and White-Light image correlation methods: Theory and experiments", Optical Society of America

[12]. L. M. Richards, S. M. Shams Kazmi, J. L. Davis , A. K. Dunn and K. E. Olin, 2010, "Low-cost Laser Speckle Contrast Imaging of blood flow using a webcam", Department of Biomedical Engineering, The University of Texas at Austin, Austin, TX

[13]. W. Dandach , J. Molimard and P. Picart, ," Direct Strain And Slope Measurement Using 3D DSPSI", LTDS, UMR 5513, École Nationale Supérieure des Mines, SMS-EMSE, CNRS, Saint-Étienne, France

[14]. P. L. Reu, and B. D. Hansche, "Digital Image Correlation combined with Electronic Speckle Pattern interferometry for 3D Deformation Measurement in Small Samples", Sandia National Laboratories, PO Box 5800, Albuquerque, NM 87185

[15]. H. Taheri, F. Delfanian and J. Du, 2013, "Wireless NDI for Aircraft Inspection", ASNT 22nd research symposium

[16]. A. Godara, D. Raabe, 2007, "Influence of fiber orientation on global mechanical behavior and mesoscale strain localization in a short glass-fiber-reinforced epoxy polymer composite during tensile deformation investigated using digital image correlation". Max planck-Institut fur Eisenforschung, Dusselsurf, Germany

[17]. Jean-Noel Perie, Silvain Calloch, Christophe Cluzel and Francois Hild, 2002, " Analysis of Multiaxial Test on a C/C composite by using Digital Image Correlation and a damage model"experimental mechanics, Vol 42, No 3

[18]. Jean Noël Périé *,1, Hugo Leclerc, Stéphane Roux, François Hild, 2009, "Digital image correlation and biaxial test on composite material for anisotropic damage law identification", International journal of solids and structures 46

[19]. F. Laurina*, J.-S. Charriera,b, D. Lévêquea, J.-F. Mairea, A. Mavela, P. Nuñeza, 2012, "Determination of the properties of composite materials thanks to digital image correlation measurements" Procedia IUTAM 4 (2012) 106 – 115

[20]. T.A. Berfield & J.K. Patel & R.G. Shimmin & P.V. Braun & J. Lambros & N.R. Sottos, 2007, "Micro- and Nanoscale Deformation Measurement of Surface and Internal Planes via Digital Image Correlation" Experimental Mechanics (2007) 47: 51–62

[21]. Hareesh Tippur and Chandru Periasamy, 2013, "A digital gradient sensor for nondestructive evaluation and stress analysis", SPI

[22]. Duane M.Reviolock, Jr,John C. Thesken, Bradley S Forsythe, 2007, "3-D Digital Image correlation of a Composite Overwrapped Pressure Vessel During Hydrostatic Pressure Tests", NASA/TM

[23]. J. Blaber, B. Adair, A. Antoniou, 2015, "Open-Source 2D Digital Image Correlation Matlab Software" Society for Experimental mechanics

[24]. Bing Pan[1,4], Kemao Qian[2], Huimin Xie[3] and Anand Asundi, 2009, " Two-dimensional digital image correlation for in-plane displacement and strain measurement: a review" Measurement Science and Technology

VITA

Graduate School
Southern Illinois University

Mahshad Mosayebi

Mahshad.mosayebi@gmail.com

Southern Illinois University Carbondale
Master of Science, Mechanical Engineering, May 2017

Southern Illinois University Carbondale
Bachelor of Science, Mechanical Engineering, March 215

Special Honors and Awards:

ASNT travel reimbursement award 2017

Thesis Title:
Digital Laser Speckle Image Correlation

Major Professor: Tsuchin. P. Chu

Publications:

1. Mosayebi. M, Karimian. S. F and Chu. T. P., "NDT using Digital Laser Speckle Image Correlation," ASNT 26th Research Symposium